Desalination and Water Treatment
www.deswater.com
doi: 10.1080/19443994.2015.1049965

57 (2016) 12585–12607
June

Taylor & Francis
Taylor & Francis Group

Adsorption of toxic Cr(VI) ions from aqueous solution by sulphuric acid modified *Strychnos potatorum* seeds in batch and column studies

K. Anbalagan[a], P. Senthil Kumar[b,*], R. Karthikeyan[c]

[a]*Department of Chemical Engineering, SRM University, Chennai 600 033, India, Tel. +91 9442088867; email: anbu74_srm@yahoo.co.in*
[b]*Department of Chemical Engineering, SSN College of Engineering, Chennai 603 110, India, Tel. +91 9884823425; email: senthilchem8582@gmail.com*
[c]*Department of Chemical Engineering, Anjalai Ammal Mahalingam Engineering College, Kovilvenni 614 403, India, Tel. +91 4423767215; email: principal@aamec.edu.in*

Received 11 January 2015; Accepted 6 May 2015

ABSTRACT

A new low-cost adsorbent such as sulphuric acid modified *Strychnos potatorum* seeds (SMSP) was employed for the removal of toxic Cr(VI) ions from aqueous solution in batch and column modes. Results showed that the removal of Cr(VI) ions could be effectively removed with the SMSP in batch operation. Adsorption of Cr(VI) ions onto SMSP followed the pseudo-first-order and Redlich–Peterson models in batch operation and Thomas model in column operation. Adsorption was more favourable at acidic pH of 2.0 with the maximum monolayer adsorption capacity of 202.7 mg/g. NaOH was a better desorbing agent with the recovery of 93.245% of Cr(VI) ions. Column studies were optimized with various parameters such as bed height (2–10 cm), Cr(VI) ions concentration (50–250 mg/L) and flow rate (5–25 mL/min). According to the fact that SMSP-based adsorption process could be a promising technology for the removal of Cr(VI) ions from wastewaters.

Keywords: Cr(VI) ions; Isotherms; Desorption; Kinetics; Thermodynamics; Thomas model

1. Introduction

The chromium finds many applications in industrial processes such as leather tanning, electroplating, steel fabrication, mining, paper, paints and pigments, dye manufacturing, aluminium conversion coating operations, inorganic chemical industries, wood preservative treatment and petroleum refining processes [1–5]. The wastewater from these industries mainly consists of the large amounts of chromium ions. If these chromium ions are not properly treated, then it causes serious pollution effects to the living environment, because, hexavalent chromium [Cr(VI)] is considered as a highly toxic, carcinogenic and mutanogenic [6–12]. The maximum permissible limit of Cr(VI) ions in drinking water as given by Bureau of Indian Standards (BIS) is 0.05 mg/L [13]. Therefore, the removal of these chromium ions from the water/wastewater is highly important.

The different traditional techniques were available for the removal of Cr(VI) ions from the wastewater which includes the chemical precipitation, filtration, electrodeposition, membrane process, ion exchange and adsorption processes. The chemical precipitation

*Corresponding author.

and chemical reduction process produces waste sludge which requires additional treatment techniques for its disposal. These processes require large number of chemicals and which is not able to completely remove the Cr(VI) ions from the wastewater because of the structure of the precipitates. The membrane process for the removal of Cr(VI) ions from the wastewater which leads to the major problems such as membrane scaling and fouling. The major drawback of the electrodeposition method is more energy intensive than the other treatment methodologies. The main disadvantage of the ion exchange process for the treatment of Cr(VI) ions containing wastewater is due to the high cost of the resin materials. Among these techniques, the adsorption process was shown to be an economic, efficient and simple operation [14–24]. Activated carbon adsorption has been proven to be the most widely and effective adsorbents for the removal of heavy metals from the water/wastewater. Its adsorption properties are mainly owing to the high surface area, high porosity, high mechanical strength and high degree of surface reactivity. Its application was restricted because of the high cost and which is difficult to recover after the treatment. To overcome these problems, the researchers are mainly focussed on the maximum removal of Cr(VI) ions by the low-cost materials which are mostly cheap and plentiful. The preparation of new and effective low-cost adsorbent is more essential for the removal of Cr(VI) ions from the water/wastewater. A number of low-cost adsorbent materials have already been used to remove the Cr(VI) ions from the wastewater which includes agricultural biowaste [25], rice straw [26], green alga [27], banana peel [28], palm flower [29], chitosan [30–32], *Aspergillus niger* [33], pine saw dust [34], saw dust [35,36], grape waste [37], wheat bran [38], fungi [39], peat [40], bentonite [41] and boehmite [41]. However, the adsorption capacity of the natural adsorbents for the removal of Cr(VI) ions was relatively low and also the regeneration ability of the natural adsorbents was found to be poor. Therefore, the adsorbent materials with strong affinity and higher adsorption capacity for the Cr(VI) ions have been synthesized by modifying the natural materials with various organic compounds which includes sulphuric acid [42], surfactant [43] and silane coupling agent [44–46].

In this research, the raw *Strychnos potatorum* (RSP) seed powders were first applied for the removal of Cr (VI) ions from the aqueous solution. The adsorption capacity of the RSP is relatively low as compared with the other natural materials. Therefore, there is a need to improve the adsorption capacity of the adsorbent for the removal of Cr(VI) ions using the sulphuric acid as a modifying agent. The first main objective of the present research was to develop a new low-cost adsorbent such as sulphuric acid modified *S. potatorum* seeds (SMSP) towards to remove the Cr(VI) ions from the aqueous solution. The adsorption system was optimized by controlling the operating parameters such as adsorbent dose, temperature, initial Cr(VI) ions concentration, solution pH, and time for the maximum removal of Cr(VI) ions in a batch mode operation. The influence of effect of different salts on the removal of Cr(VI) ions was investigated. The adsorption equilibrium and kinetic data for the removal of Cr(VI) ions by the adsorbents were analysed to investigate the adsorption thermodynamics, isotherms and kinetics in order to understand the dynamics of the adsorption process and also to predict the adsorption mechanism. The desorption of the Cr(VI) ions from the spent SMSP was recovered with the different desorbents. The second main objective of the present research was to check the efficiency of the SMSP bed column for the removal of Cr(VI) ions from the aqueous solution through continuous adsorption system. The effect of different column operating parameters such as bed height, initial Cr(VI) ions concentration and flow rate were investigated using a laboratory scale packed-bed column. The removal efficiency curves for the adsorption of Cr(VI) ions onto SMSP were analysed, and the Thomas and bed depth service time (BDST) models were also analysed to study the dynamic behaviour of the adsorption column.

2. Materials and methods

2.1. Chemicals and instruments

A stock solution of Cr(VI) ion concentrations (50 and 500 mg/L) was prepared by dissolving the measured amount of potassium dichromate ($K_2Cr_2O_7$) salt in a double-distilled water. This stock solution was diluted with double-distilled water to prepare the desired experimental Cr(VI) ions solution concentration. All the chemicals used throughout the experimental studies were of analytical grade. The solutions of 0.1N NaOH and 0.1N HCl were used to adjust the pH of the experimental solutions (pH meter, Elico Model, India). All the glassware was rinsed with 0.1N HCl solutions, and then, it was washed with double-distilled water to remove the adsorbed metal ions on the glass wall. The concentration of the Cr(VI) ions in the solution was measured using atomic absorption spectrometer (AAS, SL176 Model, Elico Limited, Chennai, India).

2.2. SMSP preparation

The *S. potatorum* seeds were collected from the Pudukkottai District, Tamilnadu, India, to prepare

the surface modified *S. potatorum* seeds using concentrated sulphuric acid (dehydration process). The collected seeds were washed with adequate tap water to remove the impurities. The washed materials were dried in sunlight, and then, this was made into powder using conventional mixer grinder. The prepared materials were abbreviated as raw *S. potatorum* seeds (RSP). The required amounts (say 25 g) of dried RSP were treated with the required amount of concentrated sulphuric acid of 16 mol/L (1:2 ratio of RSP to acid) to increase the adsorption properties of the adsorbent, and this reaction mixtures were kept in a dark room for about 24 h. The excess acid present in the reaction mixtures was removed by repeated washing with double-distilled water until the supernatant pH reached the value of 7.0. The collected wet solid materials were completely dried at 80˚C in the hot-air oven. The dried solid materials were ground into a fine powder using conventional mixer grinder, and then, it was sieved to obtain the average particle size of 0.354 mm. This prepared material was abbreviated as sulphuric modified *S. potatorum* seeds (SMSP), and this material was utilized as an adsorbent for the removal of Cr(VI) ions from the aqueous solution.

2.3. Scanning electron microscopic (SEM) analysis

The surface morphology of the RES and SMES was measured using a Quanta 200 FEG scanning electron microscope at an accelerating voltage of 30 kV and with the working distance of 100 μm was used.

2.4. Point of zero charge (PZC) measurement

The measured amount of SMSP (2.5 g) was placed in a 50-mL conical flask along with 25 mL of double-distilled water. This mixture was agitated in a temperature-controlled incubation shaker, and the pH of the solution was tested continuously until a constant pH value was obtained. The PZC of the adsorbent was calculated by mass titration method suggested by Noh and Schwas [47]. The different initial solution pH (2.0–10.0) was prepared using 0.1N NaOH and 0.1N HCl. The five conical flasks of 50 mL capacities were filled with 15 mL of the different pH solution and with the different amounts of SMSP (0.1–5%). The mixtures were agitated in a temperature-controlled incubation shaker for about 24 h, and the equilibrium pH was measured and which was plotted against mass fraction. The PZC of the SMSP is the point at which the change of the pH is zero.

2.5. Batch adsorption methods

Batch adsorption methods were carried out for the removal of Cr(VI) ions from the aqueous solution using RSP and SMSP, as an adsorbents. Based on the batch adsorption results, the efficient adsorbent will be tested for the column adsorption methods. Batch adsorption experiments were performed in a stoppered conical flask agitated in a temperature-controlled incubation shaker (180 rpm) at different adsorbent dose (0.5–4.0 g/L), different temperatures (30–60˚C), different contact time (0–90 min), different pH values (2.0–4.0) and at different initial Cr(VI) ion concentrations (5–500 mg/L) to optimize the adsorption process parameters to get the maximum removal of Cr(VI) ions. An aqueous solution with a volume of 100 mL of known Cr(VI) ion concentration was taken in the 100 mL of a stoppered conical flask along with the measured amount of adsorbent dose. This adsorption system was kept in a temperature-controlled incubation shaker at 180 rpm. The samples were carried out at an appropriate time intervals, and then, the supernatant/spent adsorbent was separated using centrifugation operation. The residual concentration of Cr(VI) ions in the solution was measured using AAS. The removal of Cr(VI) ions from the aqueous solution for the known initial Cr(VI) ions concentration was calculated by the following relationship:

$$\% \text{ Removal} = \frac{C_0 - C_e}{C_0} \times 100 \quad (1)$$

where C_0 and C_e are the initial and final or equilibrium Cr(VI) ions concentrations (mg/L), respectively.

2.5.1. Batch thermodynamic studies

In this adsorption experimental study, the aqueous solution temperature was varied from 30 to 60˚C in order to estimate the thermodynamic parameters. The experiments were carried out in series of 100-mL stoppered conical flasks at different temperatures in a temperature-controlled incubation shaker. The samples were withdrawn at specific time intervals, and then, it was analysed for the measurement of Cr(VI) ions concentration in the solution using AAS. Adsorption thermodynamics are essential to estimate whether the process is a spontaneous or not and also to check the process is an exothermic or an endothermic. The negative value of Gibb's free energy (ΔG°) indicates the adsorption process is a spontaneous in nature of adsorption. The adsorption thermodynamic parameters such as Gibb's free energy (ΔG°), enthalpy change

(ΔH°) and entropy change (ΔS°) were evaluated from the following equation:

$$\Delta G = -RT \ln\left(\frac{C_{Ae}}{C_e}\right) \tag{2}$$

$$\log\left(\frac{C_{Ae}}{C_e}\right) = \frac{\Delta S}{2.303\,R} - \frac{\Delta H}{2.303\,RT} \tag{3}$$

where R is the gas constant (8.314 J/mol/K), T is the temperature (K), C_{Ae} is the amount of Cr(VI) ions adsorbed onto the adsorbent per L of solution at equilibrium (mg/L), and C_e is the equilibrium concentration of Cr(VI) ions in the solution (mg/L).

2.5.2. Batch equilibrium studies

It is most important to predict the best adsorption isotherm equation for the equilibrium curve to optimize the design of a batch adsorption system. The removal of the metal ions from the aqueous solution by the adsorbent highly depends on the initial solution pH of the adsorption system. The influence of solution pH on the removal of Cr(VI) ions was studied by applying the adsorption equilibrium data to the different adsorption isotherm models. In the adsorption isotherm experimental study, the aqueous solution pH was varied from 2.0 to 4.0 in order to check the influence of the solution pH on the removal of Cr (VI) ions. The adsorption isotherm experiments were carried out in series of 100 mL stoppered conical flasks at different pH values for the different initial Cr(VI) ions concentration in a temperature-controlled incubation shaker. The samples were withdrawn from the adsorption system after the system was reached equilibrium time. The adsorption mixtures were separated by centrifugation operation, and then, the supernatant was analysed for the residual concentration of Cr(VI) ions in the solution using AAS. The amount of Cr(VI) ions adsorbed onto the SMSP at equilibrium time, q_e (mg/g), was calculated by the following equation:

$$q_e = \frac{(C_o - C_e)\,V}{m} \tag{4}$$

where q_e is the equilibrium adsorption capacity (mg/g), V is the volume of Cr(VI) ions solution, and m is the mass of adsorbent (g).

In this study, the two-parameter (Langmuir [48] and Freundlich [49]) and the three-parameter (Redlich–Peterson [50] and Sips [51]) adsorption isotherm models were applied to fit the adsorption equilibrium data. The non-linear regression analysis was performed to estimate the parameters, R^2 and error values using MATLAB R2009a software. The results of the analysis can able to predict the best adsorption isotherm models for the obtained equilibrium curve.

Langmuir model [48]:

$$q_e = \frac{q_m K_L C_e}{1 + K_L C_e} \tag{5}$$

where q_m is the maximum monolayer adsorption capacity of the adsorbent (mg/g), and K_L is the Langmuir constant related to the affinity of the Cr(VI) ions to the adsorbent (L/mg).

Freundlich model [49]:

$$q_e = K_F C_e^{1/n} \tag{6}$$

where K_F is the Freundlich constant ((mg/g)(L/mg)$^{(1/n)}$) related to the bonding energy, n is a measure of the deviation from linearity of adsorption (g/L). The significance of "n" is as follows: $n = 1$ (linear); $n < 1$ (chemical process); $n > 1$ (physical process).

Redlich–Peterson model [50]:

$$q_e = \frac{K_{RP} C_e}{1 + \alpha_{RP} C_e^{\beta_{RP}}} \tag{7}$$

where K_{RP} is Redlich–Peterson isotherm constant (L/g), α_{RP} is Redlich–Peterson isotherm constant (L/mg)$^{1/\beta}{}_{RP}$, and β_{RP} is the exponent which lies between 0 and 1. The importance of "β" is as follows: $\beta = 1$ (Langmuir adsorption isotherm model is a preferable adsorption isotherm model); $\beta = 0$ (Freundlich adsorption isotherm model is a preferable adsorption isotherm model).

Sips model [51]:

$$q_e = \frac{K_S C_e^{\beta_S}}{1 + \alpha_S C_e^{1/\beta_S}} \tag{8}$$

where K_S is the Sips model constant (L/g)$^{\beta s}$, α_S is the Sips isotherm constant (L/g)$^{1/\beta s}$, and β_S is the Sips model exponent. The constant β_S is often considered as the heterogeneity factor. The significance of β_S is as follows: $\beta_S > 1$ (heterogeneous adsorption system); $\beta_S = 1$ (a material with relatively homogenous binding sites). For $\beta_S = 1$, the Sips model reduces to the Langmuir model equation.

2.5.3. Batch kinetic studies

The adsorption kinetic studies were performed in a series of stoppered conical flasks with 100 mL of known concentration of Cr(VI) ions solutions along with the adsorbents (RSP and SMSP) and by varying the contact time from 10 to 90 min, while keeping the other operating parameters (adsorbent dosage, solution pH, different initial Cr(VI) ions concentration and temperature) constant. The adsorption mixtures were then agitated in a temperature-controlled incubation shaker at 180 rpm. At predetermined time interval, the samples were withdrawn and it was analysed for the measurement of Cr(VI) ions using AAS. The amount of Cr(VI) ions adsorbed onto the SMSP at different time intervals, q_t (mg/g), was calculated using the following equation:

$$q_t = \frac{(C_o - C_t)V}{m} \tag{9}$$

where q_t is the amount of Cr(VI) ions adsorbed onto the adsorbent at any time t (mg/g), C_t is the concentration of the Cr(VI) ions measured at any time t (mg/L), V is the volume of the Cr(VI) ions solution (L), and m is the mass of the biosorbent (g).

In order to evaluate the rate of adsorption and the rate-controlling mechanism in the removal of Cr(VI) ions by the adsorbents (RSP and SMSP), the adsorption kinetic data were modelled using pseudo-first-order, pseudo-second-order, and Elovich kinetic models.

Pseudo-first-order kinetic model [52]:

$$q_t = q_e(1 - \exp(-k_1 t)) \tag{10}$$

where k_1 is the pseudo-first-order kinetic rate constant (min^{-1}), and t is the time (min).

Pseudo-second-order kinetic model [53]:

$$q_t = \frac{q_e^2 k_2 t}{1 + q_e k_2 t} \tag{11}$$

where k_2 is the pseudo-second-order kinetic rate constant (g/mg.min).

Elovich kinetic model [54]:

$$q_t = (1 + \beta_E)\ \ln(1 + \alpha_E\ \beta_E t) \tag{12}$$

where β_E (g/mg) is the desorption constant related to the extent of the surface coverage and activation energy for chemisorption, and α_E is the initial adsorption rate in mg/(g min). The non-linear regression analysis was carried out to evaluate the kinetic parameters, equilibrium adsorption capacity, R^2 and error values using MATLAB R2009a software. The results of the kinetic analysis can able to predict the suitable adsorption kinetic model for the obtained kinetic data.

2.5.4. Effect of different salts

The effect of different salts such as NH_4Cl, NH_4NO_3, KNO_3, $MgSO_4$, $NaHCO_3$, and $K_2P_2O_7$ on the removal of Cr(VI) ions was tested by taking 100 mL of Cr(VI) ions concentration of 100 mg/L along with an optimum amount of SMSP in a stoppered conical flask with the presence of the above-mentioned salts. This adsorption mixtures where shaken in a temperature-controlled incubation shaker at 180 rpm for about 2 h. After that, the adsorption mixtures were separated using centrifugation operation and the supernatant was analysed for residual Cr(VI) ions concentration using AAS.

2.6. Batch desorption methods

The spent adsorbent was collected from the different batch adsorption experimental studies. The measured amount of spent adsorbent was taken in a series of stoppered conical flasks along with the known concentration of 100 mL of different desorbents (0.1N H_2SO_4, 0.1N HCl, 0.1N HNO_3, 10% HCHO, 0.1N KOH and 0.1N NaOH). This system was agitated in a temperature-controlled incubation shaker at 180 rpm for about 2 h. After this time duration, the spent adsorbent-desorbing agent system mixtures were separated by centrifugation operation. The recovered concentration of Cr(VI) ions in the supernatant was analysed by AAS. The recovery of Cr(VI) ions was calculated using the following equation:

$$\%\ \text{of Cr(VI) ions recovery} = \frac{\text{amountofCr(VI) ionsdesorbed}}{\text{amount of Cr(VI) ions adsorbed}} \times 100 \tag{13}$$

2.7. Column adsorption methods

Column adsorption methods were performed for the removal of Cr(VI) ions from the aqueous solution using SMSP as an effective adsorbent. Column adsorption tests were conducted in a vertical packed-bed column with varying the different operating parameters such as different bed height (2–10 cm), different

initial Cr(VI) ions concentration (50–250 mg/L) and at different flow rates (5–25 mL/min) to optimize the column adsorption process parameters to know the maximum removal of Cr(VI) ions. The adsorption column was packed with an adequate amount of SMSP to obtain the required bed height of the adsorbent (2–10 cm) and keep the flow rate constant (5 mL/min) and by varying the different influent Cr (VI) ions concentration (50–250 mg/L). The effluent sample was collected at regular time intervals to estimate the residual Cr(VI) ions concentration using AAS. The flow of the influent was continued until there was no further adsorption in the column process. The Cr(VI) ions concentration in the effluent was used to estimate the adsorption capacity of the SMSP.

2.8. Column adsorption data analysis

The removal of Cr(VI) ions by the SMSP in the adsorption column was represented in the mass transfer zone of the breakthrough curves. At initially, the maximum removal of Cr(VI) ions by the SMSP was observed, and after that, it was gradually changed with the time until the breakthrough curve was obtained. The breakthrough curves were attained by plotting C/C_0 against t; where C is the concentration of Cr(VI) ions at the exit of the adsorption column (mg/L), C_o is the initial concentration of Cr(VI) ions at the inlet of the adsorption column (mg/L), and t is the service time (min). The adsorption column was analysed for the removal of Cr(VI) ions at different bed heights (2, 4, 6, 8 and 10 cm), at different initial Cr(VI) ions concentration (50, 100, 150, 200 and 250 mg/L) and at different flow rates (5, 10, 15, 20 and 25 mL/min). The treated effluent volume (V_t) was calculated as follows:

$$V_t = Q\, t_{total} \tag{14}$$

where Q is the volumetric flow rate (mL/min), and t_{total} is the total flow time (min).

The maximum column adsorption capacity (q_{total}, mg) for a given Cr(VI) ions concentration of feed and the flow rate are the measure of the area under the plot of the concentration of Cr(VI) ions adsorbed. This can be expressed as follows:

$$q_{total} = \frac{QA}{1,000} = \frac{Q}{1,000}\int_{t=0}^{t=total} C_{ad}\, dt \tag{15}$$

where Q is the volumetric flow rate (mL/min), A is the area under the breakthrough curve, and $C_{ad} = (C_o - C_t)$ is the concentration of Cr(VI) ions adsorbed (mg/L).

Maximum adsorption capacity or equilibrium adsorption capacity of the column (q_e, mg/g) is expressed as follows:

$$q_{eq} = \frac{q_{total}}{m} \tag{16}$$

where m is the dry weight of the adsorbent in the adsorption column (g). The total amount of Cr(VI) ions entered into the adsorption column (m_{total}) is calculated as follows [55]:

$$W_{total} = \frac{C_o\, Q\, t_{total}}{1,000} \tag{17}$$

The percentage removal of Cr(VI) ions can be calculated as follows:

$$Y\% = \frac{q_{total}}{W_{total}} \tag{18}$$

The removal efficiency of Cr(VI) ions was calculated as follows:

$$\%\ \text{Removal efficiency} = 1 - \frac{C}{C_0} \times 100 \tag{19}$$

where C_o and C are the initial and final concentration of Cr(VI) ions solution (mg/L), respectively.

2.8.1. Thomas model

Thomas model [56] is the most general and widely used adsorption models in describing the adsorption column performance and prediction of breakthrough curves. Thomas model assumes plug flow behaviour in the adsorption bed. Theoretically, it is useful to determine the adsorption process where the internal and external diffusion resistances were extremely small and they will not be the rate limiting steps in the adsorption process. If the adsorption process is explained by the pseudo-second-order kinetic rate principle, then, it is reduced to a Langmuir isotherm equation at equilibrium condition. The expression developed by Thomas is used for the determination of the maximum solid phase concentration of the solute on the adsorbent, q_o, and the adsorption rate constant, k_{th}. The linearized form of this model is represented as follows:

$$\ln\left[\left(\frac{C_0}{C}\right) - 1\right] = \left(\frac{k_{th} q_o m}{F}\right) - k_{th} C_o t \tag{20}$$

where C_o and C are the input and output concentrations in the adsorption column (mg/L), respectively, q_o is the maximum solid phase concentration (mg/g), k_{th} is the Thomas rate constant ($Lmg^{-1}\,h^{-1}$), m is the amount of adsorbent (g) in the column, and F is the volumetric flow rate ($Lmin^{-1}$).

2.8.2. BDST model

The analysis of the breakthrough curve was further carried out using the BDST model [57]. The BDST model is used to discuss the adsorption bed capacity of the adsorbent with the help of the different breakthrough values. It is the easiest method used in the adsorption system design. This model is used in the calculation of the relationship between bed depth, Z, and service time at breakthrough, t_b. A linear relationship between the bed depth (Z) and service time (t) in terms of process concentrations and adsorption parameters is represented as follows:

$$\ln\left(\frac{C_o}{C_b}-1\right)=\ln(e^{k_aN_oZ/v}-1)-k_aC_ot \tag{21}$$

Hutchins [57] proposed a linear relationship between the bed height (Z) and service time (t) given as follows:

$$t=\left(\frac{N_a}{C_0v}\right)Z-\frac{1}{k_aC_0}\ln\left(\frac{C_0}{C_b}-1\right) \tag{22}$$

where C_0 is the influent concentration of Cr(VI) ions (mg/L), C_b is the breakthrough Cr(VI) ion concentration (mg/L), i.e. the effluent Cr(VI) ions concentration reached 5% of the total influent Cr(VI) ions concentration, N_a is the adsorption capacity of the bed (mg/L), v is the linear velocity (cm/min), and k_a is the rate constant (L/mg.min). The model constants k_a and N_a can be determined from the plot of Z against t of the above equation.

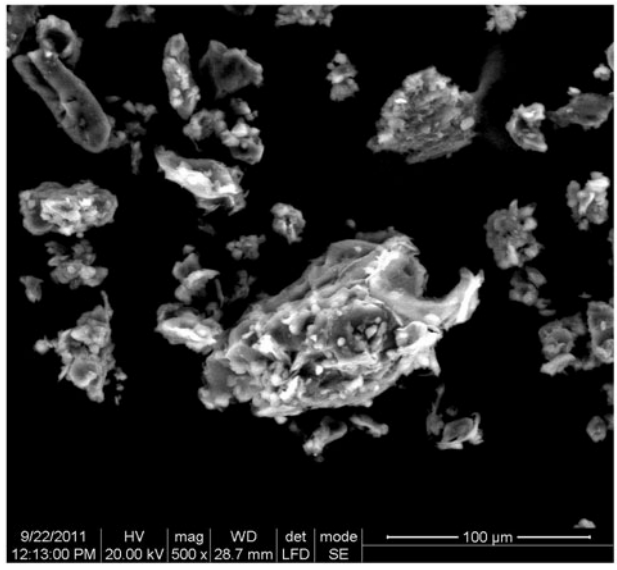

Fig. 1a. SEM image of RSP.

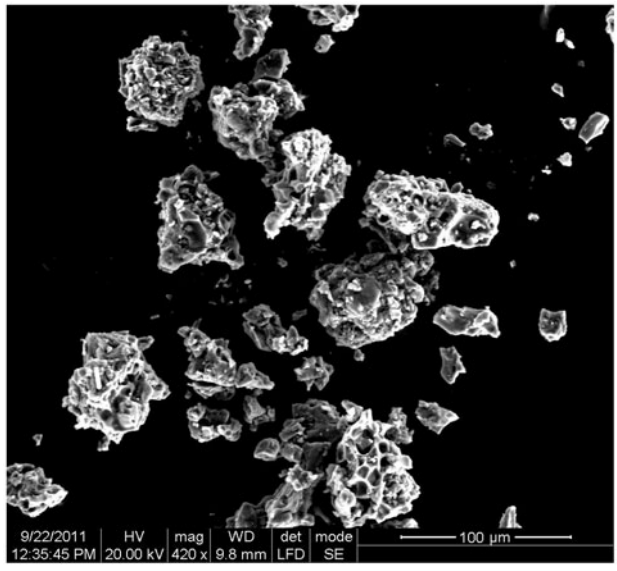

Fig. 1b. SEM image of SMSP.

3. Results and discussion

3.1. Characterization of the S. potatorum seeds

SEM analysis was used to identify the surface morphology of the adsorbent materials. The SEM images of the RSP and SMSP were shown in Figs. 1(a) and (b), respectively. From Fig. 1(a), it was observed that the RSP surface had a uniform surface morphology but the surface of the RSP was much more irregular in shape. The SEM image of RSP also shows that there are no pores present on its surface. The RSP particles were treated with sulphuric acid to modify its surface and which creates more pores on the treated particles, i.e. SMSP surface. This was clearly showed in Fig. 1(b). From Fig. 1(b), it can be seen that the irregular pores were developed on the SMSP surface because of the action of sulphuric acid on the RSP which indicates the formation of different sizes of the distributed pores. Based on the SEM analysis, it can be concluded that the SMSP has a more adequate morphology for

the removal of Cr(VI) ions than the RSP particles. The Fourier transform infrared spectroscopic analyses of the adsorbents (RSP and SMSP) were discussed in our previous research work [22].

The pH value of the SMSP solution was found to be of 3.95 at a solid-to-liquid water ratio of 1:1 (w/v). The PZC of the SMSP was measured as 3.5. The pH value which is less than 3.5 indicates that the surface of the SMSP is positively charged and the net negative charge will be observed above the pH value of 3.5.

3.2. Batch adsorption studies

3.2.1. Effect of adsorbent types and dose

The effect of adsorbent types (RSP and SMSP) and the adsorbent dose for the removal of Cr(VI) ions from the aqueous solution were carried out, and the results were shown in Figs. 2(a) and (b). Fig. 2 shows that the removal of Cr(VI) ions was increased with the increase in adsorbent dose but the equilibrium adsorption capacity was decreased with the increase in adsorbent dose. The removal of Cr(VI) ions was almost constant beyond 3 (for RSP) and 2 g/L (for SMSP). This may be due to the increase in the active sites of the adsorbent with the increase in adsorbent dose, and the maximum removal was observed at an optimum dose of 3 (for RSP) and 2 g/L (for SMSP). The equilibrium adsorption capacity was found maximum at 3 (for RSP) and 2 g/L (for SMSP), and then, declining trend was observed at higher doses of the adsorbent. This may be due to the availability of the more active sites for the lower adsorbent dose and overlapping or aggregation of the adsorption sites at higher adsorbent dosages. The initial increase in the equilibrium adsorption capacity can be due to the increase in the adsorbent surface area and the availability of the more adsorption sites. It may also be explained that at higher adsorbent dosages, the available Cr(VI) ions were not enough to cover all the active sites of the adsorbent which indicates the lower Cr(VI) ions uptake capacity. The results show that the SMSP is suitable for higher initial Cr(VI) ion concentrations because of its effectiveness but the RSP is suitable only for lower initial Cr(VI) ion concentrations.

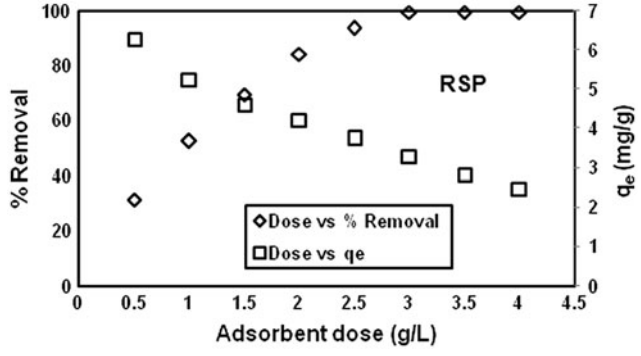

Fig. 2a. Effect of adsorbent dose on the removal of Cr(VI) ions by RSP [Cr(VI) ions concentration = 10 mg/L, pH 2.0, volume of sample = 100 mL, equilibrium time = 60 min and temperature 30°C].

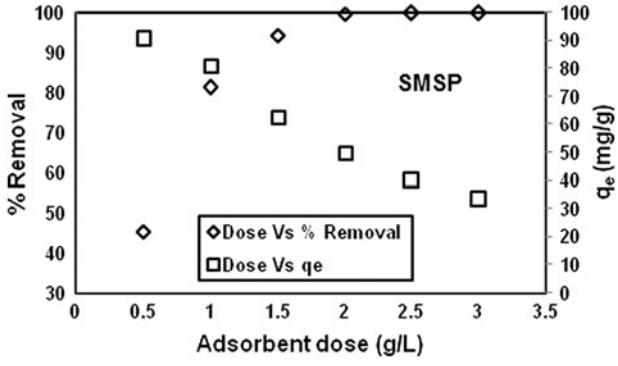

Fig. 2b. Effect of adsorbent dose on the removal of Cr(VI) ions by SMSP [Cr(VI) ions concentration = 100 mg/L, pH 2.0, volume of sample = 100 mL, equilibrium time = 30 min and temperature 30°C].

3.2.2. Effect of temperature

The effect of temperature on the removal of Cr(VI) ions by the adsorbents (RSP and SMSP) was investigated by varying the temperatures from 303 to 333 K, and the results were shown in Figs. 3(a) and (b). From Fig. 3, it was observed that the removal of Cr(VI) ions was decreased with the increase in temperature. The results indicated that the temperature highly influenced the adsorption of Cr(VI) ions onto the adsorbents. The maximum removal of Cr(VI) ions by the adsorbents was obtained at 30°C. The removal of Cr(VI) ions and equilibrium adsorption capacity (not shown) was decreased sharply with the increase in temperature. The decrease in the removal of Cr(VI) ions and the equilibrium adsorption capacity indicates that the lower temperature favours the removal of Cr(VI) ions by the adsorbents. The adsorption of Cr(VI) ions from the aqueous solution phase onto the solid–liquid interface occurs by eject the water from the interfacial region. The solution viscosity was decreased with the rise in temperature which appeared to be more favourable for the transfer and diffusion of the Cr(VI) ions from the bulk solution to the adsorbent surface. But the removal of Cr(VI) ions was decreased with the increase in temperature might be due to the desorption of Cr(VI) ions from the adsorbent surface at higher temperature.

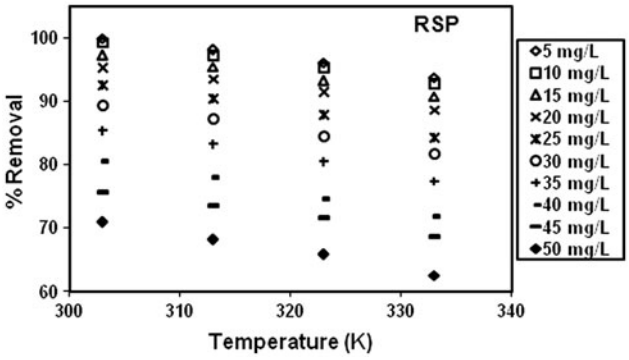

Fig. 3a. Effect of temperature on the removal of Cr(VI) ions by RSP [Cr(VI) ions concentration = 5–50 mg/L, pH 2.0, adsorbent dose = 3 g/L, volume of sample = 100 mL and equilibrium time = 60 min].

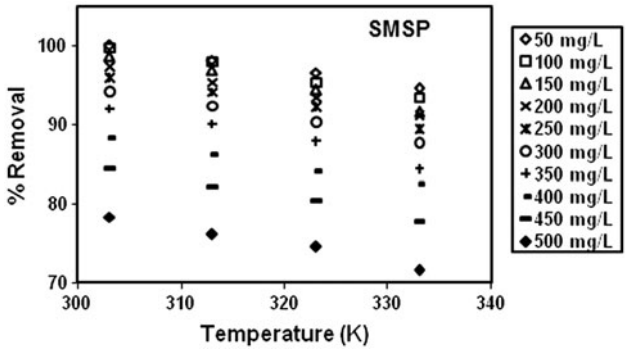

Fig. 3b. Effect of temperature on the removal of Cr(VI) ions by SMSP [Cr(VI) ions concentration = 50–500 mg/L, pH 2.0, adsorbent dose = 2 g/L, volume of sample = 100 mL and equilibrium time = 30 min].

It is also possible that as the temperature increases, the denaturation of the active sites of the adsorbents also increases. This process indicates that the adsorption of Cr(VI) ions onto the adsorbents was exothermic process.

3.2.3. Adsorption thermodynamics

The adsorption mechanism was explained by estimating the adsorption thermodynamic parameters such as Gibbs free energy change (ΔG°), enthalpy change (ΔH°) and entropy change (ΔS°). The value of ΔG° is calculated from Eq. (2), and it was listed in Tables 1 (for RSP) and 2 (for SMSP). The values of ΔH° and ΔS° were calculated from the slopes and intercepts of the plots of log K_c vs. $1/T$ [Fig. 4(a) for RSP and Fig. 4(b) for SMSP], and these were listed in Tables 1 (for RSP) and 2 (for SMSP). The negative values of ΔG° confirm the feasibility of the adsorption process and the spontaneous nature of the adsorption process with a high preference of Cr(VI) ions onto the adsorbents. The values of ΔG° was decreased with the increase in temperature which indicate that the affinity of Cr(VI) ions onto the adsorbents was higher at a lower temperature. The significance of the ΔG° value is: −20 to 0 kJ/mol (physical process) and −80 to −400 kJ/mol (chemical process). The values of ΔG° for the present adsorption process were between −20 and 0 kJ/mol which indicates that the adsorption of Cr(VI) ions onto the adsorbent was a physical process. The value of ΔH° was found to be positive which indicates that the adsorption of Cr(VI) ions onto the adsorbents was exothermic in nature which may be due to the weak interaction between the adsorbent and Cr(VI) ions. The negative value of ΔS° suggests a decrease in the randomness at the solid/solution interface during the adsorption process.

3.2.4. Adsorption isotherms

Adsorption isotherm is the relationship between the amounts of solute adsorbed per gram of the adsorbent as a function of the equilibrium concentration in the solution at constant temperature. The adsorption isotherm study was carried out with the help of the data obtained from the effect of initial Cr(VI) ions concentration and the solution pH studies. The removal of Cr(VI) ions from the aqueous solution by the adsorbents was dependent on the initial concentration of Cr (VI) ions. At low Cr(VI) ions concentration, the ratio of the available surface to the initial concentration of Cr(VI) ions was larger which indicates that the removal of Cr(VI) ions was found to be high. However, at higher Cr(VI) ions concentration, this ratio was low; hence, the removal of Cr(VI) ions was also found to be lower. The equilibrium adsorption capacity was increased with the increase in initial Cr(VI) ions concentration which may be due to the increased rate of mass transfer and which indicates the increased concentration of driving force. The removal of Cr(VI) ions by the adsorbents is highly depends on the pH of the adsorption system. The influence of the solution pH on the removal of Cr(VI) ions was determined by applying the adsorption equilibrium data to the most widely used adsorption isotherm models such as two-parameter (Langmuir and Freundlich) adsorption isotherm models and the three-parameter (Redlich–Peterson and Sips) adsorption isotherm models, and the fitted models were shown in Figs. 5–8. The calculated parameters from these models were listed in Tables 3 (for RSP) and 4 (for SMSP). The solution pH affects the net negative charge on the adsorbent surface, physico-chemistry and hydrolysis

Table 1
Adsorption thermodynamic parameters for the removal of Cr(VI) ions by RSP

Conc. of Cr(VI) ions solution (mg/L)	ΔH° (kJ/mol)	ΔS° (J/mol/K)	ΔG° (kJ/mol)			
			30℃	40℃	50℃	60℃
5	−118.942	−339.096	−17.993	−10.239	−8.607	−7.516
10	−63.511	−170.773	−12.320	−9.274	−8.113	−7.102
15	−36.609	−91.274	−9.054	−7.941	−7.052	−6.325
20	−26.863	−63.530	−7.619	−6.973	−6.375	−5.699
25	−23.244	−55.642	−6.346	−5.873	−5.324	−4.667
30	−17.636	−40.439	−5.364	−5.006	−4.572	−4.158
35	−15.086	−35.001	−4.454	−4.166	−3.794	−3.408
40	−13.577	−33.009	−3.558	−3.278	−2.891	−2.586
45	−9.662	−22.402	−2.851	−2.664	−2.473	−2.162
50	−10.362	−26.749	−2.245	−1.976	−1.769	−1.418
			K_c values			
5			1,264.823	51.138	24.654	15.101
10			133.048	35.298	20.515	13.004
15			36.383	21.148	13.819	9.820
20			20.584	14.581	10.739	7.836
25			12.417	9.553	7.261	5.396
30			8.408	6.847	5.489	4.489
35			5.860	4.958	4.108	3.424
40			4.107	3.524	2.935	2.545
45			3.101	2.783	2.512	2.184
50			2.438	2.137	1.932	1.669

Table 2
Adsorption thermodynamic parameters for the removal of Cr(VI) ions by SMSP

Conc. of Cr(VI) ions solution (mg/L)	ΔH° (kJ/mol)	ΔS° (J/mol/K)	ΔG° (kJ/mol)			
			30℃	40℃	50℃	60℃
50	−128.382	−367.051	−19.357	−10.340	−8.961	−7.919
100	−92.347	−258.295	−15.107	−10.143	−8.119	−7.347
150	−51.812	−136.423	−10.673	−8.917	−7.569	−6.608
200	−35.192	−86.622	−9.113	−7.864	−7.140	−6.492
250	−28.739	−68.547	−8.019	−7.218	−6.671	−5.920
300	−23.091	−52.942	−7.049	−6.488	−6.029	−5.436
350	−20.966	−48.749	−6.159	−5.754	−5.325	−4.667
400	−13.271	−27.055	−5.098	−4.779	−4.484	−4.299
450	−11.089	−24.949	−4.250	−3.974	−3.782	−3.481
500	−9.832	−21.694	−3.242	−3.022	−2.888	−2.559
			K_c values			
50			2,172.913	53.171	28.138	17.471
100			402.226	49.302	20.561	14.209
150			69.175	30.766	16.756	10.879
200			37.241	20.533	14.281	10.434
250			24.132	16.021	11.989	8.486
300			16.416	12.098	9.444	7.123
350			11.533	9.126	7.263	5.397
400			7.565	6.274	5.400	4.726
450			5.404	4.605	4.089	3.516
500			3.621	3.194	2.931	2.519

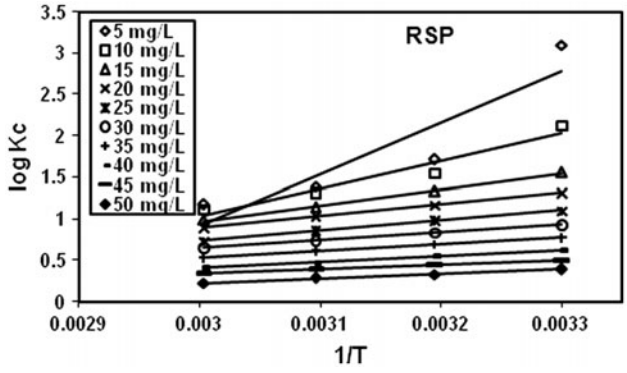

Fig. 4a. Adsorption thermodynamics for the removal of Cr (VI) ions by RSP [Cr(VI) ions concentration = 5–50 mg/L, pH 2.0, adsorbent dose = 3 g/L, volume of sample = 100 mL and equilibrium time = 60 min].

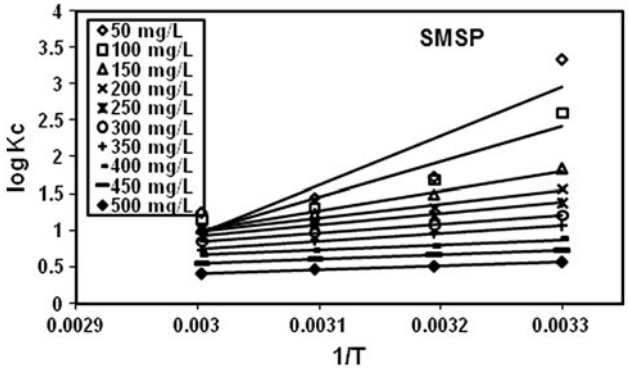

Fig. 4b. Adsorption thermodynamics for the removal of Cr (VI) ions by SMSP [Cr(VI) ions concentration = 50–500 mg/L, pH 2.0, adsorbent dose = 2 g/L, volume of sample = 100 mL and equilibrium time = 30 min].

of the Cr(VI) ions. This is highly important to predict the optimum solution pH for the maximum removal of Cr(VI) ions. It was observed from the Tables 3 and 4, the adsorption capacity of the adsorbents for the removal of Cr(VI) ions was found to be decreased with the increase in the solution pH. The higher adsorption capacity was observed at the strong acidic pH condition which indicates that the electrostatic attraction between the negatively charged chromium species and the positively charged adsorbent surface. At these very low pH ranges or high acidic pH ranges, the functional groups will be protonated due to the excess availability of H^+ ions. The low adsorption capacity value was observed at the pH value of 4.0, and the maximum adsorption capacity value was observed at a pH value of 2.0. From these results, it was observed that the optimum solution pH for the maximum removal of Cr(VI) ions was 2.0.

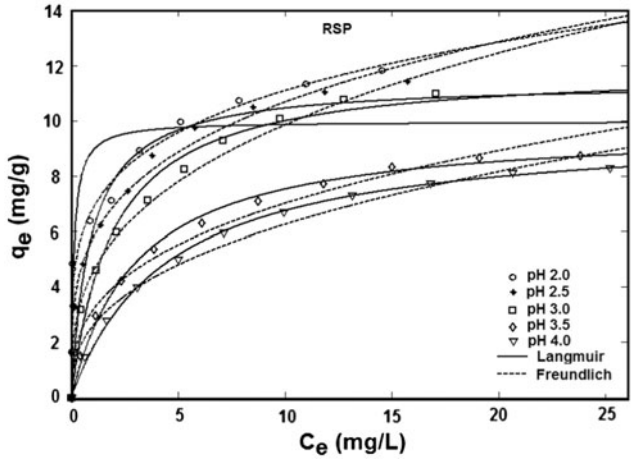

Fig. 5. Two-parameter adsorption isotherm models for the removal of Cr(VI) ions by RSP [Cr(VI) ions concentration = 5–50 mg/L, pH 2.0, adsorbent dose = 3 g/L, volume of sample = 100 mL and equilibrium time = 60 min].

In the adsorption isotherm study, the two-parameters (Langmuir and Freundlich) and the three-parameters (Redlich–Peterson and Sips) adsorption isotherm models were employed to fit the adsorption equilibrium data of the adsorption of Cr(VI) ions onto adsorbents (RSP and SMSP). These adsorption isotherm models were tested using the MATLAB R2009a software to calculate the adsorption isotherm parameters, error function values (SSE, Sum of Squared Error and RMSE, Root Mean Squared Error) and coefficient of determination (R^2) values at different solution pH conditions. These values were estimated from the plot of C_e vs. q_e (Figs. 5–8), and these values were listed in Tables 3 and 4. The high R^2 and low error values were chosen as the best fitted adsorption isotherm model with the adsorption equilibrium data than the other adsorption isotherm models. The experimental adsorption isotherms followed a general trend that the equilibrium adsorption capacity (q_e) was increased with the increase in the equilibrium Cr(VI) ions concentration (C_e) and it was reached the saturation value at higher equilibrium concentrations at all studied different solution pH conditions. The L-shaped isotherm curves observed which indicates that the ratio between the equilibrium concentration of Cr(VI) ions (C_e) and the equilibrium adsorption capacity (q_e) decreases when the Cr(VI) ions concentration increased, which gave a concave curve.

The Langmuir adsorption isotherm parameters (q_m and K_L), R^2 values and error (SSE and RMSE) values were calculated from the plot of q_e vs. C_e (Figs. 5 and 7)at 30℃, and the values were given in Tables 3 and 4. The separation parameter (R_L) values gave the

Table 3
Isotherm constants of two-parameters and three-parameters models for the removal of Cr(VI) ions by the RSP

	Two-parameters model constants					
Adsorption isotherm models	pH	2.0	2.5	3.0	3.5	4.0
Langmuir	q_m (mg/g)	11.92	11.39	9.972	9.806	9.738
	K_L (L/mg)	8.459	1.115	0.521	0.3309	0.226
	R^2	0.844	0.9553	0.9812	0.9959	0.9985
	SSE	25.65	6.934	2.695	0.373	0.1214
	RMSE	1.688	0.8778	0.5472	0.2036	0.1162
Freundlich	K_F [(mg/g)(L/mg)$^{(1/n)}$)]	6.822	5.757	4.532	3.165	2.596
	n (g/L)	4.739	3.73	2.965	2.893	2.617
	R^2	0.9798	0.9916	0.9882	0.9787	0.9795
	SSE	3.32	1.299	1.684	1.933	1.641
	RMSE	0.6073	0.3799	0.4325	0.4634	0.427
Three-parameters model constants						
Redlich–Peterson	K_{RP} (L/g)	3,749	145.3	18.17	4.447	2.571
	a_{RP} (L/mg)$^{(1/\ \beta RP)}$	543.5	23.47	2.977	0.6573	0.34
	β_{RP}	0.7947	0.762	0.7662	0.8841	0.9245
	R^2	0.9802	0.9948	0.9963	0.9986	0.9992
	SSE	3.256	0.8008	0.5253	0.1254	0.0678
	RMSE	0.6379	0.3164	0.2563	0.1252	0.09201
Sips	K_S (L/g)$^{\beta s}$	5,844	264.3	25.35	4.748	2.595
	a_s (L/mg)$^{(\beta s)}$	846.9	43.59	4.501	0.771	0.37
	β_S	1.108	1.13	1.136	1.072	1.047
	R^2	0.9803	0.9945	0.9958	0.9984	0.999
	SSE	3.232	0.8595	0.5946	0.1489	0.0833
	RMSE	0.6356	0.3278	0.2726	0.1364	0.102

important details on the nature of adsorption process, i.e. favourable or unfavourable or linear or irreversible. The importance of R_L values are as follows: $R_L = 0$ (irreversible), $0 < R_L < 1$ (favourable), $R_L = 1$ (linear) or $R_L > 1$ (unfavourable). The separation parameter (R_L) values were calculated from the Langmuir adsorption isotherm parameters. The R_L values for the present adsorption system presented between 0 and 1 which indicates that the adsorption process is a favourable adsorption [58]. The Freundlich adsorption isotherm parameters (K_F and n), R^2 values, error (SSE and RMSE) values were estimated from the plot of q_e vs. C_e (Figs. 5 and 7) at 30˚C, and these values were given in Tables 3 and 4. From Tables 3 and 4, it can be seen that the n value was observed between 1 and 10 which recommend that the adsorption of Cr(VI) ions onto the adsorbents is a physical process [59]. Based on the high value of R^2 and low error values, the Freundlich adsorption isotherm model was most suitable than the Langmuir adsorption isotherm model for the present adsorption system. The overall results showed that both Langmuir and Freundlich adsorption isotherm models best fits the adsorption equilibrium data and indicates that both monolayer and heterogeneous surface properties exit at studied experimental conditions. The three-parameter (Redlich–Peterson and Sips) adsorption isotherm model parameters, R^2 values and error (SSE and RMSE) values were calculated from the plot of q_e vs. C_e (Figs. 6 and 8) at 30˚C, and the values were listed in Tables 3 and 4. The three-parameter adsorption isotherm models explain the adsorption equilibrium data are better than the two-parameter adsorption isotherm models because of the additional parameter in the three-parameter model and also due to the complexity in nature. Among the studied adsorption isotherm models, Sips model gave the best fit to the adsorption equilibrium data based on the higher R^2 and low error values. The Redlich–Peterson adsorption isotherm parameters (K_{RP}, a_{RP} and β_{RP}), R^2, error (SSE and RMSE) values were estimated from the plot of q_e vs. C_e (Figs. 6 and 8) at 30˚C, and the values were presented in Tables 3 and 4. The Redlich–Peterson model exponent (β_{RP}) values were appeared to be closer to unity, suggests that the data follow the Langmuir model. The Sips adsorption isotherm parameters (K_S, a_s and β_S), R^2 and error (SSE and RMSE) values were calculated from the plot of q_e vs. C_e (Figs. 6 and 8) at 30˚C, and the values were given in Tables 3 and 4. In the present adsorption isotherm study, the Sips

Table 4
Isotherm constants of two-parameters and three-parameters models for the removal of Cr(VI) ions by the SMSP

	Two-parameters model constants					
Adsorption isotherm models	pH	2.0	2.5	3.0	3.5	4.0
Langmuir	q_m (mg/g)	202.7	195.1	172.3	147.4	132.3
	K_L (L/mg)	0.2054	0.0626	0.04	0.03947	0.03517
	R^2	0.9387	0.9715	0.9883	0.991	0.9985
	SSE	2,835	1,156	332.1	194.5	26.13
	RMSE	17.75	11.33	6.075	4.648	1.704
Freundlich	K_F [(mg/g)(L/mg)$^{(1/n)}$)]	69.02	37.27	26.48	23.7	21.23
	n (g/L)	4.242	2.905	2.859	2.997	3.076
	R^2	0.9906	0.9958	0.9873	0.9841	0.9707
	SSE	432.8	168.5	358.6	341.3	496.2
	RMSE	6.935	4.327	6.312	6.158	7.425
Three-parameters model constants						
Redlich–Peterson	K_{RP} (L/g)	5,618	140.6	15.35	10.4	5.448
	a_{RP} (L/mg)$^{(1/\ \beta RP)}$	79.61	3.26	0.2761	0.1766	0.0581
	β_{RP}	0.7699	0.686	0.788	0.8312	0.938
	R^2	0.9911	0.997	0.9969	0.999	0.9994
	SSE	411.6	119.8	88.24	22.06	9.809
	RMSE	7.173	3.87	3.321	1.661	1.107
Sips	K_S (L/g)$^{\beta s}$	10,001	202.4	14.73	9.518	5.128
	a_s (L/mg)$^{(\beta s)}$	142.6	4.98	0.3152	0.1879	0.0601
	β_S	1.122	1.176	1.128	1.101	1.039
	R^2	0.991	0.9968	0.9962	0.9988	0.9994
	SSE	414.7	130.1	107	24.84	10.08
	RMSE	7.2	4.033	3.657	1.762	1.123

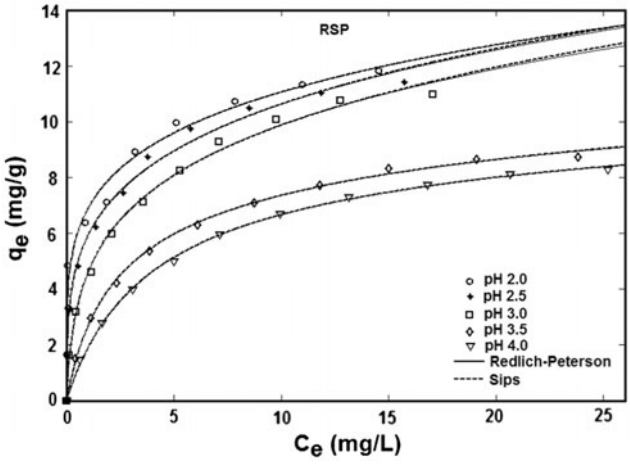

Fig. 6. Three-parameter adsorption isotherm models for the removal of Cr(VI) ions by RSP [Cr(VI) ions concentration = 5–50 mg/L, pH 2.0, adsorbent dose = 3 g/L, volume of sample = 100 mL and equilibrium time = 60 min].

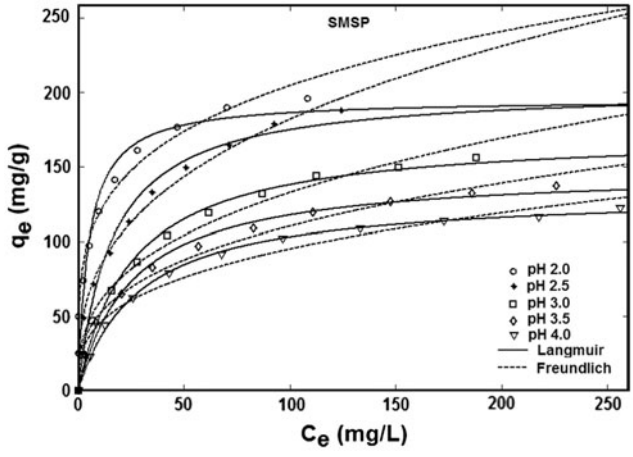

Fig. 7. Two-parameter adsorption isotherm models for the removal of Cr(VI) ions by SMSP [Cr(VI) ions concentration = 50–500 mg/L, pH 2.0, adsorbent dose = 2 g/L, volume of sample = 100 mL and equilibrium time = 30 min].

adsorption isotherm model gave relatively high R^2 values and low error values. The Sips adsorption isotherm model exponent (β_S) values were noticed to be closer to unity which observes that the adsorption equilibrium data follow the Langmuir adsorption isotherm model [60]. The successful explanation of the adsorption equilibrium data by the Sips adsorption isotherm model indicates that the adsorption of Cr(VI) ions onto the adsorbents followed the heterogeneous process. The comparison of the maximum monolayer

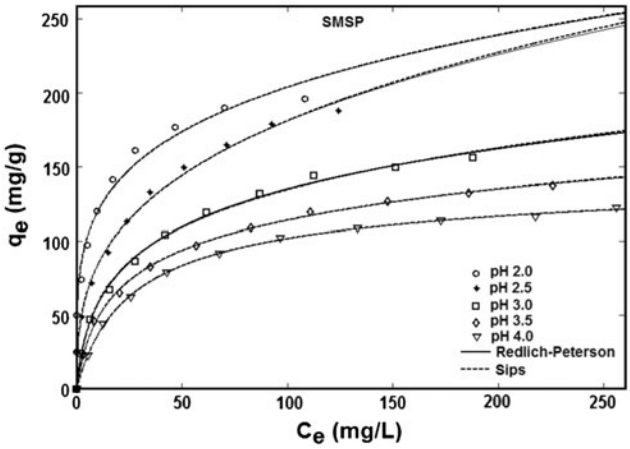

Fig. 8. Three-parameter adsorption isotherm models for the removal of Cr(VI) ions by SMSP [Cr(VI) ions concentration = 50–500 mg/L, pH 2.0, adsorbent dose = 2 g/L, volume of sample = 100 mL and equilibrium time = 30 min].

adsorption capacity of the SMSP for the removal of Cr (VI) ions was compared with the other adsorbents, and it was presented in Table 5. From Table 5, it was observed that the maximum value was observed for SMSP as compared with the other adsorbents.

3.2.5. Adsorption kinetics

The adsorption rate for the removal of metal ions by the adsorbents is most important while designing the batch adsorption experiments. Also, it is highly significant to establish the time dependence of the adsorption systems under different process conditions. The adsorption experimental results for the removal of Cr(VI) ions by the adsorbents (RSP and SMSP) were shown in Figs. 9 (for RSP) and 10 (for SMSP). This result revealed that the adsorption of Cr(VI) ions was fast and the equilibrium was achieved within 60 min of contact time for RSP and 30 min of contact time for SMSP. The time for reaching the equilibrium condition was slightly increased with the increase in initial concentration of the Cr(VI) ions. The Cr(VI) ions uptake was increased with the increase in initial Cr(VI) ions

Table 5
Comparison of maximum monolayer adsorption capacity of the SMSP with other adsorbents for the removal of Cr (VI) ions

Adsorbents	q_m(mg/g)	References
SMSP seeds	202.7	This study
Chemically modified coir pith	196	[61]
Unmodified coir pith	165	[61]
Commercial activated carbon	153.96	[61]
Durian shell waste	117	[62]
Prawn shell activated carbon	100.60	[63]
Cupressus lusitanica bark	87.5	[64]
Activated lignin	77.8	[65]
Cotton fibre	69.15	[66]
Activated carbon (Filtrasorb-400)	57.70	[63]
Sulfonated lignite	27.87	[3]
Activated charcoal	12.87	[67]
RSP seeds	11.92	This study
Coir pith carbon	10.9	[68]
Coal	6.78	[69]
AC derived from coconut shells	1.38	[70]

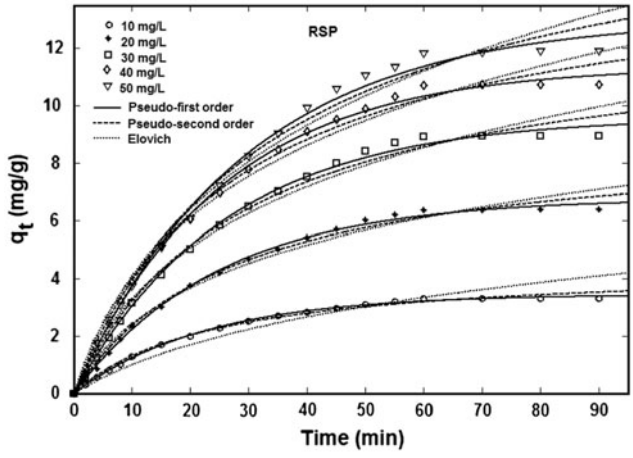

Fig. 9. Adsorption kinetics for the removal of Cr(VI) ions by RSP [Cr(VI) ions concentration = 10–50 mg/L, pH 2.0, adsorbent dose = 3 g/L, volume of sample = 100 mL and temperature = 30°C].

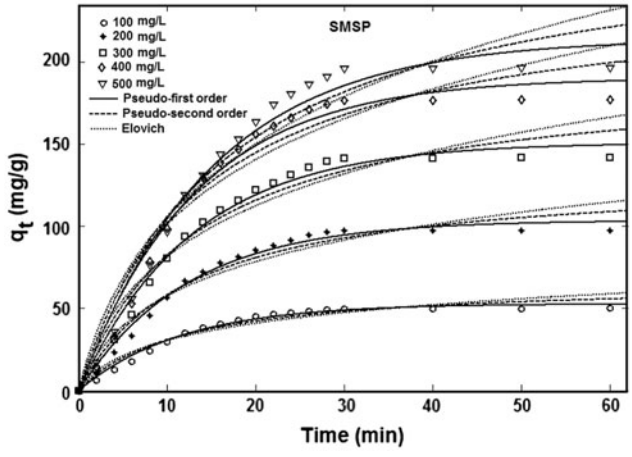

Fig. 10. Adsorption kinetics for the removal of Cr(VI) ions by SMSP [Cr(VI) ions concentration = 100–500 mg/L, pH 2.0, adsorbent dose = 2 g/L, volume of sample = 100 mL and temperature = 30°C].

concentration. This may be due to an increase in the initial concentration of the Cr(VI) ions contributing a larger driving force to overcome all the mass transfer resistances between the solid and the liquid phase which results in the higher adsorption of Cr(VI) ions. At initial time period, the higher adsorption of Cr(VI) ions was observed. This may be due to the availability of more number of active sites which results in an increased concentration gradient between the Cr(VI) ions in the aqueous solution and the Cr(VI) ions on the adsorbent surface. If the time for the adsorption process was increased further then the concentration gradient was reduced because of the adsorption of Cr (VI) ions onto the active sites of the adsorbent. This result suggested that the adsorption process was reduced at the later stages.

The various adsorption kinetic models have been applied to explain the removal of metal ions from the aqueous solution, whereas the most widely used are pseudo-first-order, pseudo-second-order and Elovich kinetic models. To evaluate the adsorption kinetics and rate-controlling mechanism in the removal of Cr (VI) ions by the adsorbents, the adsorption kinetic data were modelled using the different adsorption kinetic models such as the pseudo-first-order, pseudo-second-order and Elovich kinetic models. The adsorption kinetic results were shown in Figs. 9 (for RSP) and 10 (for SMSP). The kinetic results indicated that the pseudo-first-order kinetic model provides the best fit to the adsorption kinetic data with the high R^2 and low error values than the other models (Table 6 for RSP and Table 7 for SMSP). From Tables 6 and 7, it was observed that the R^2 values for the pseudo-first-order kinetic model were close to one and the calculated value of q_e also agreed with the experimental q_e value. This confirms that the adsorption of Cr(VI) ions onto the adsorbents followed the pseudo-first-order kinetic model. It was also observed that the R^2 values for the pseudo-second-order kinetic model were found to be low and the huge difference between the calculated q_e and experimental q_e values. Therefore, the adsorption of Cr(VI) ions onto the adsorbents (RSP and SMSP) does not follow the pseudo-second-order kinetic model. The obtained R^2 values for the Elovich kinetic model were found to be lower than that of the pseudo-first-order and pseudo-second-order kinetic equations. The Elovich kinetic model does not guess any definite mechanism for the removal of Cr(VI) ions, but it is helpful in explaining the adsorption of Cr(VI) ions onto the highly heterogeneous adsorbents. This Elovich model may also be used to guess the adsorption kinetics for the entire adsorption period because all the adsorbents (RSP and SMSP) possess the heterogeneous surface active sites.

3.2.6. Effect of different salts

Generally, the chromium-contaminated industrial wastewaters consist of different types of salts along with the chromium. These salts may disturb the removal of Cr(VI) ions from the wastewater by the adsorbent (SMSP). Hence, the effect of different salts

Table 6
Adsorption kinetic parameters for the removal of Cr(VI) ions by RSP

		Concentration of Cr(VI) ion solution (mg/L)				
Kinetic model	Parameters	10	20	30	40	50
Pseudo-first-order equation	k_1 (min^{-1})	0.04449	0.04301	0.03842	0.03971	0.03428
	$q_{e,}$ cal (mg/g)	3.451	6.774	9.603	11.38	13.04
	R^2	0.9988	0.9976	0.9973	0.9978	0.996
	SSE	0.02873	0.2203	0.4943	0.568	1.298
	RMSE	0.04111	0.1138	0.1705	0.1828	0.2763
Pseudo-second-order equation	k_2 (g/mg.min)	0.00929	0.004019	0.00262	0.00235	0.001616
	$q_{e,}$cal (mg/g)	4.47	8.958	12.83	15.07	17.8
	$q_{e,}$exp (mg/g)	3.421	6.453	9.104	10.825	11.984
	R^2	0.9947	0.9925	0.9918	0.9936	0.9909
	SSE	0.1259	0.6866	1.493	1.647	2.928
	RMSE	0.08606	0.201	0.2963	0.3112	0.415
Elovich kinetic equation	α (mg/g.min)	127.3	1.014	0.2015	0.1578	0.07809
	β (g/mg)	0.0004267	0.1488	0.675	0.9368	1.405
	R^2	0.9305	0.9832	0.9829	0.9852	0.9838
	SSE	1.64	1.535	3.12	3.781	5.222
	RMSE	0.3106	0.3005	0.4284	0.4716	0.5543

Table 7
Adsorption kinetic parameters for the removal of Cr(VI) ions by SMSP

Kinetic model	Parameters	Concentration of Cr(VI) ion solution (mg/L)				
		100	200	300	400	500
Pseudo-first-order equation	k_1 (min^{-1})	0.08677	0.08162	0.07806	0.07658	0.0672
	$q_{e,}$ cal (mg/g)	52.78	103.5	150.9	190.3	214.1
	R^2	0.9871	0.9869	0.9864	0.9785	0.9799
	SSE	61.51	241.3	530.3	1,382	1,584
	RMSE	1.902	3.768	5.585	9.018	9.653
Pseudo-second-order equation	k_2 (g/mg.min)	0.001308	0.000606	0.000387	0.000293	0.000213
	$q_{e,}$cal (mg/g)	66.4	131.6	193.3	245.7	282.5
	$q_{e,}$exp (mg/g)	49.992	97.632	141.852	177.156	196.537
	R^2	0.9629	0.9643	0.9651	0.9544	0.9593
	SSE	176.5	655.7	1,364	2,939	3,210
	RMSE	3.222	6.211	8.958	13.15	13.74
Elovich kinetic equation	α (mg/g.min)	0.07313	0.02875	0.01681	0.01187	0.007504
	β (g/mg)	6.531	14.33	21.97	28.71	34.73
	R^2	0.9287	0.9329	0.9357	0.9232	0.9343
	SSE	339.3	1,232	2,513	4,942	5,185
	RMSE	4.467	8.514	12.16	17.05	17.46

(NH_4Cl, NH_4NO_3, KNO_3, $MgSO_4$, $NaHCO_3$ and $K_2P_2O_7$) and control (Cr(VI) ions alone) on the removal of Cr(VI) ions by the SMSP was investigated, and the results were shown in Fig. 11. From Fig. 11, it was observed that the presence of the sulphate ions (SO_4^{2-}) decreases the removal of Cr(VI) ions. It was indicated that the high level of SO_4^{2-} will increase the reduction of Cr(VI) ions to the Cr(III) ions. This may be attributed to the SO_4^{2-} does not act as a competitive electron acceptor in the reduction of Cr(VI) ions to the Cr(III) ions by the adsorbent [26,61]. For the present adsorption system, the removal of Cr(VI) ions was decreased because of the competition between the SO_4^{2-} and the chromate/dichromate ions towards the active sites of the adsorbent and which indicates that both Cr(III) and Cr(VI) ions were adsorbed onto the adsorbent. It was observed that only less influence of the NH_4Cl, NH_4NO_3 and KNO_3 on the removal of Cr (VI) ions by the SMSP. The presence of dissolved NO^{3-} in the solution may control the removal of Cr (VI) ions and the reduction of Cr(VI) ions to the Cr (III) ions. Further, it was also observed that the removal of Cr(VI) ions was decreased with the presence of $NaHCO_3$ and $K_2P_2O_7$ salts because of the competition between CO_3^{2-} and $P_2O_7^{2-}$ with the Cr(VI) ions to the active sites of the adsorbent. The observed results from the effect of different salts were compared with the control, and the results are shown in Fig. 11. It was concluded that the presence of other salts hinders the removal of Cr(VI) ions from the aqueous solution by the SMSP.

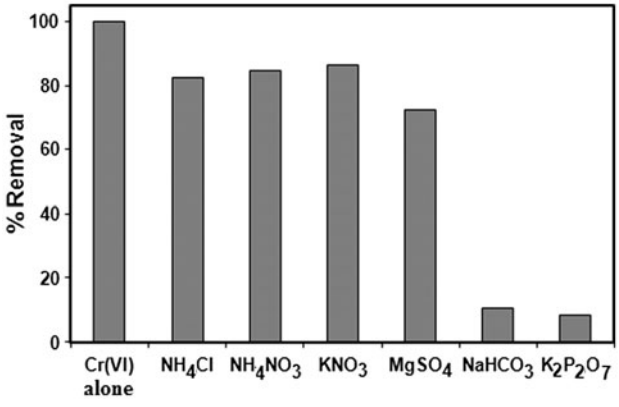

Fig. 11. Effect of different salts on the removal of Cr(VI) ions by SMSP.

3.3. Batch desorption studies

The effect of different desorbents such as 0.1N H_2SO_4, 0.1N HCl, 0.1N HNO_3, 10% HCHO, 0.1N KOH and 0.1N NaOH on the recovery of Cr(VI) ions from the spent SMSP were carried out to identify the best desorbing agents, and the results were shown in Fig. 12. From Fig. 12, it was observed that the recovery of Cr(VI) ions from the spent adsorbent was found to be maximum while using NaOH as a desorbing agent as compared with the other desorbing agents. KOH also showed some positive results for the recovery of Cr(VI) ions from the spent adsorbent. The recovery of Cr(VI) ions from the spent adsorbent by other desorbents such as H_2SO_4, HCl, HNO_3 and HCHO

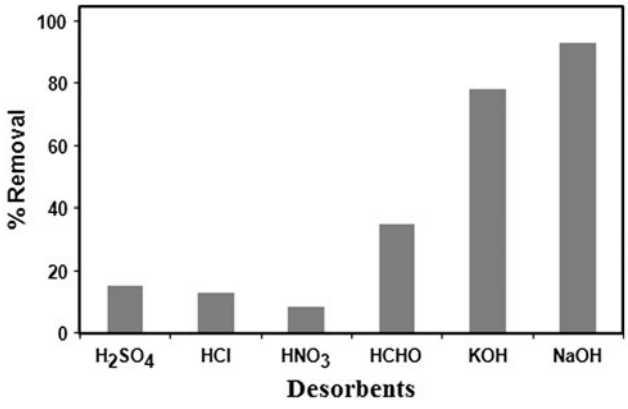

Fig. 12. Desorption results on the recovery of Cr(VI) ions from spent SMSP.

was found to be low. The most efficient desorbing agent was 0.1N NaOH and which was recovered nearly 93.245% of Cr(VI) ions from the spent SMSP. Another desorbing agent such as 0.1N KOH showed the recovery of Cr(VI) ions from the spent SMSP was about 78.362%. The reason may be due to the reduction in the electrostatic attraction between the Cr(VI) ions and the SMSP because of the effect of alkaline medium such as 0.1N NaOH and KOH solutions [65]. The complete recovery of the Cr(VI) ions from the spent adsorbent is not possible because of the non-electrostatic forces between the Cr(VI) ions and the SMSP [71,72].

3.4. Column adsorption studies

The performance of the SMSP in a fixed packed-bed column is an important factor to access the feasibility of the SMSP in the real industrial wastewater treatment processes. The adsorption studies in a fixed packed-bed column were carried out in a glass column (40 cm height and 3 cm inner diameter) which consists of a known measured quantity of SMSP. The arrangement of fixed packed-bed column was shown in Fig. 13. All the experimental studies were carried out at 30˚C. For all the experimental studies, the adsorption column was packed with the known quantity of SMSP for the required bed height (2–10 cm), at different constant flow rate (5–25 mL/min) and the known initial Cr(VI) ions concentration (50–250 mg/L) having the pH value of 2.0 which was pumped from top to the bottom through the adsorption column with the help of peristaltic pump. The 0.1N HCl was used to adjust the pH of the treatment solution. At predetermined time intervals, the samples were collected and it was analysed for the residual Cr(VI) ions concentration using the AAS.

3.4.1. Effect of bed height

The effect of bed height on the removal of Cr(VI) ions by the SMSP at pH 2.0, 50 mg/L of Cr(VI) ions solution, 5 mL/min flow rate and at a constant temperature of 30˚C was investigated, and the results

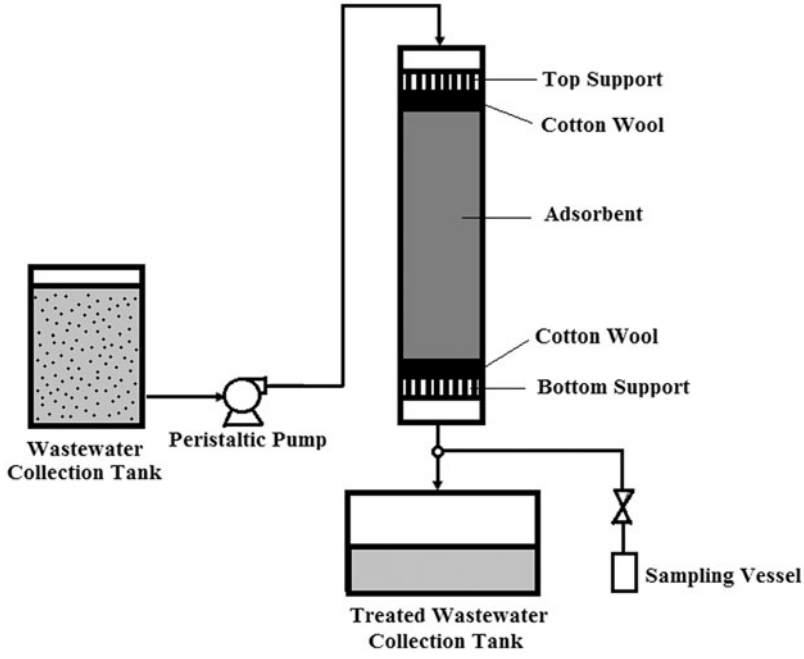

Fig. 13. Schematic diagram of a continuous flow fixed-bed column.

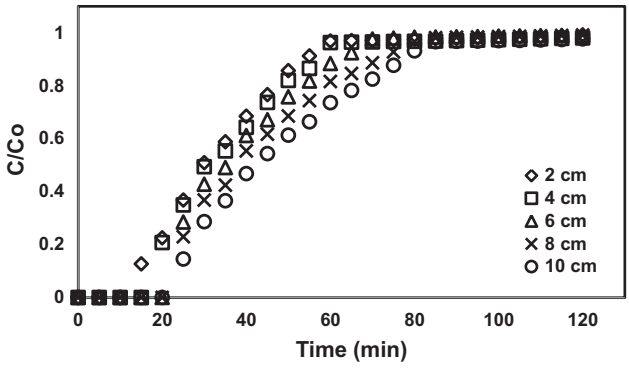

Fig. 14. Effect of bed height on the adsorption of Cr(VI) ions onto SMSP.

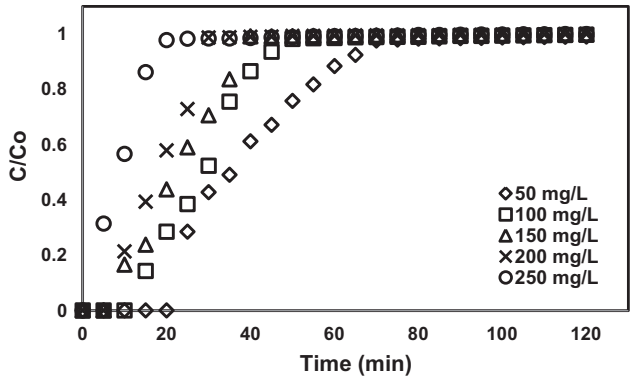

Fig. 15. Effect of initial Cr(VI) ion concentration on the adsorption of Cr(VI) ions onto SMSP.

were shown in Fig. 14. From Fig. 14, it was observed that the breakthrough and exhaustion times were extended with increase in bed heights which may be due to the longer bed heights which allows a longer empty bed contact time between the Cr(VI) ions and the SMSP. The movement of the Cr(VI) ions in the packed-bed column may be due to the axial and longitudinal distribution of the Cr(VI) ions in the packed-bed column. It was also observed that the slope of the breakthrough curve became flatter with the increase in bed heights which provide in a broadened mass transfer zone. The adsorption column was required much longer time to reach the complete exhaustion. At low bed height, only a less number of active sites were available to remove the Cr(VI) ions from the aqueous solution which indicates that the SMSP was saturated at faster rate and the breakthrough was achieved earlier. At higher bed height, the more number of active sites for the adsorption of Cr(VI) ions by the SMSP was observed because of the longer breakthrough time and more volume of treated water. For the present adsorption system, the sufficient or optimum bed height for the removal of Cr(VI) ions from the aqueous solution was found to be of 6 cm.

3.4.2. Effect of influent Cr(VI) ions concentration

The effect of various influent concentration of Cr(VI) ions (50–250 mg/L) on the adsorption of Cr(VI) ions onto SMSP at pH 2.0, bed height of 6 cm, 5 mL/min flow rate and at a constant temperature of 30˚C was studied, and the results were shown in Fig. 15. The breakthrough curves were obtained at five different initial Cr(VI) ion concentrations (50–250 mg/L) by plotting the experimental data between C/C_0 and t (Fig. 15). It was found that the breakthrough time was decreased with the increase in initial concentration of Cr(VI) ions. It was also found that the adsorption capacity was increased with the increase in the influent concentration of Cr(VI) ions. This may attributed to the reduction in length of adsorption zone by enhancing the Cr(VI) ions concentration which improved the adsorption rate of Cr(VI) ions.

3.4.3. Effect of flow rate

The influent flow rate plays an important role for the evaluation of the adsorption capacity of the adsorbent in the continuous treatment of industrial wastewater. The effect of different flow rates (5–25 mL/min) on the adsorption of Cr(VI) ions onto SMSP at pH 2.0, 50 mg/L of Cr(VI) ions solution, bed height of 6 cm and at a constant temperature of 30˚C was investigated, and the results were shown in Fig. 16. The breakthrough curves were obtained at five different flow rates by plotting the experimental data between C/C_o and t (Fig. 16). The breakthrough curves showed that the adsorption capacity was decreased with the increase in the influent flow rate. It

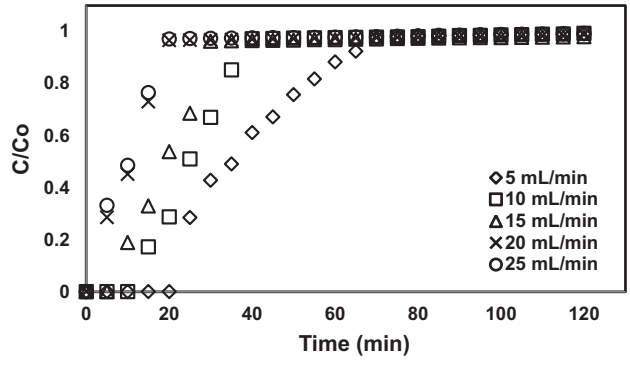

Fig. 16. Effect of flow rate on the adsorption of Cr(VI) ions onto SMSP.

may be due to the shorter residential time was given for the adsorption and also the diffusion process at the high value of flow rate in the adsorption column. It was also observed that the breakthrough time for the present adsorption system was decreased with the increase in the flow rate. This may be attributed to the improvement in the speed of the adsorption region at higher flow rate which causes the reduction in the time necessary to reach the required breakthrough concentration. The sufficient or optimum flow rate for the present adsorption system was found to be of 5 mL/min.

3.5. Thomas model

The Thomas model is mostly used to estimate the maximum solid phase concentration of the solute on the adsorbent (q_o, mg/g) and the adsorption rate constant (k_{th}, $Lmg^{-1}\ min^{-1}$). The values of q_o and k_{th} were estimated by applying the adsorption column data from the effects of bed height, influent Cr(VI) ions concentration and influent flow rate to the Thomas model (Figs. 17–19). The values of q_o and k_{th} were calculated by plotting the adsorption column data between $\ln[(C_0/C)-1]$ and t, and the results were given in Table 8. The best fit of the adsorption column data to the Thomas model was checked on the basis of highest R^2 values. From Table 8, it was observed that the q_o values were increased from 0.5635 to 1.991 mg/g and the value of k_{th} reduced from 0.00214 to 0.00144 $Lmg^{-1}\ min^{-1}$ by increasing the bed heights from 2 to 10 cm. It was also observed that the q_o values were increased from 0.7488 to 1.5267 mg/g and the value of k_{th} reduced from 0.0018 to 0.001052 $Lmg^{-1}\ min^{-1}$ by increasing the influent Cr(VI) ions concentration from 50 to 250 mg/L. The contradictory results were observed for the influent flow rate on the column adsorption experimental studies. From Table 8, it can be seen that the q_o values were decreased from 0.7488 to 0.5642 mg/g and the value of k_{th} increased from 0.0018 to 0.00482 $Lmg^{-1}\ min^{-1}$ by increasing the influent flow rate from 5 to 25 mL/min. The results showed that the Thomas model best fitted on the bed heights, influent Cr(VI) ion concentrations and flow rates.

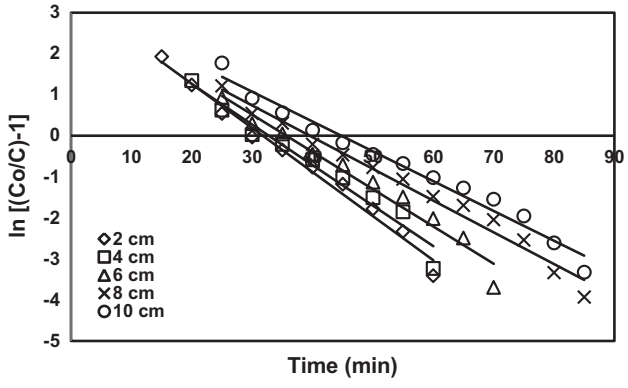

Fig. 17. Thomas model fit for the adsorption of Cr(VI) ions onto SMSP at different bed heights.

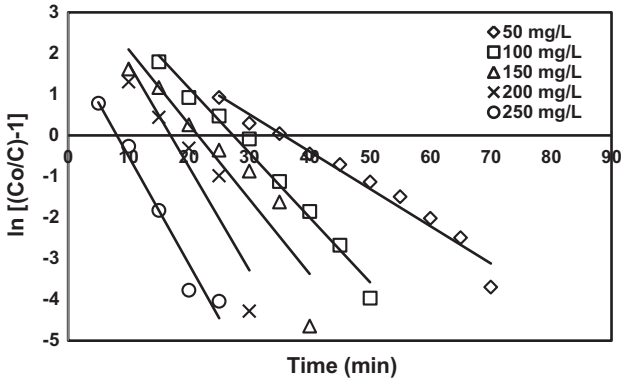

Fig. 18. Thomas model fit for the adsorption of Cr(VI) ions onto SMSP at different initial Cr(VI) ions concentration.

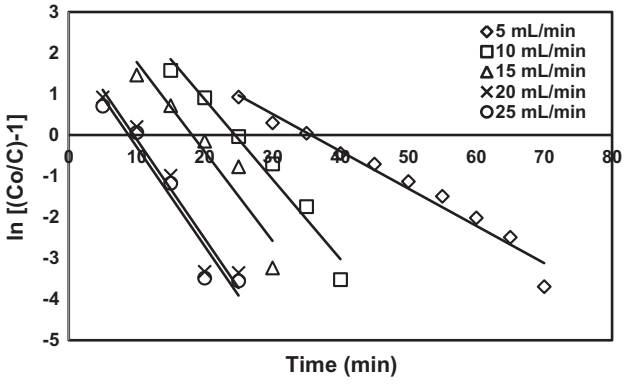

Fig. 19. Thomas model fit for the adsorption of Cr(VI) ions onto SMSP at different flow rate.

3.6. BDST model

The BDST model provides the information on the linear relationship among the bed depth (Z) and service time (t_b). The adsorption column data were applied to the BDST model, and the plots were drawn between Z and t_b values. The result of the BDST model was shown in Fig. 20. The values of N_a and k_a were calculated from the slope and the intercept of the plot of Z and t_b values (Fig. 20). For a given linear flow rate, the curve Z vs. t_b was found to be linear

Table 8
Thomas model parameters for the adsorption of Cr(VI) ions onto SMSP at different conditions

Bed depth (cm)	Flow rate (mL/min)	Initial Cr(VI) ions concentration (mg/L)	q_o (mg/g)	k_{th} (Lmg^{-1} min^{-1})	R^2
2	5	50	0.5635	0.00214	0.984
4	5	50	0.6201	0.00196	0.974
6	5	50	0.7488	0.0018	0.982
8	5	50	1.031	0.00154	0.980
10	5	50	1.991	0.00144	0.975
6	5	100	0.8585	0.00157	0.985
6	5	150	1.3481	0.00126	0.912
6	5	200	1.4173	0.00121	0.924
6	5	250	1.5267	0.001052	0.964
6	10	50	0.7128	0.00388	0.979
6	15	50	0.6857	0.00434	0.914
6	20	50	0.5921	0.00476	0.934
6	25	50	0.5642	0.00482	0.935

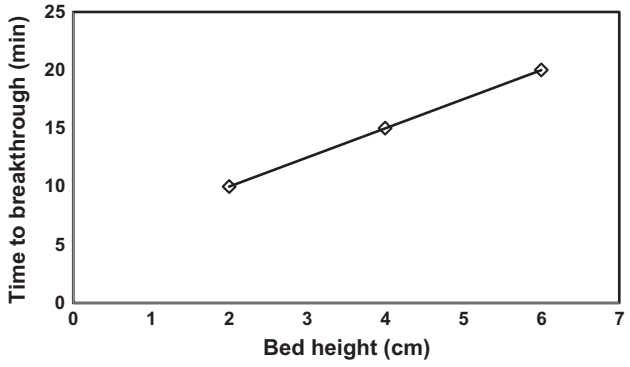

Fig. 20. BDST model fit for the adsorption of Cr(VI) ions onto SMSP.

which suggests that the BDST model applied to the present adsorption system was found to be valid ($R^2 = 1$). The values of N_a and k_a were found to be 625 and 0.01557 L/mg.min. The advantage of the BDST model is used to scale up for other flow rates without further experimental run.

4. Conclusions

The SMSP was prepared, and it was successfully applied in batch and column adsorption for the removal of Cr(VI) ions from the aqueous solution. The effectiveness of the SMSP for the removal of Cr(VI) ions was compared with the RSP seeds, and the results indicated that the SMSP showed better adsorption properties than the RSP. The present investigations showed that the SMSP can be used as a potential low-cost adsorbent for the removal of Cr(VI) ions from the aqueous solution. The results of the present investigation can be summarized as follows:

(i) In batch adsorption process, the influencing operating parameters such as adsorbent dose, temperature, solution pH, initial Cr(VI) ions concentration and time were optimized for the maximum removal of Cr(VI) ions from the aqueous solution. The predicted optimum conditions for the batch mode operations are of solution pH 2.0, SMSP dose = 2.0 g/L, equilibrium time = 30 min and temperature = 30°C.
(ii) Acidic solution pH was more favourable for the removal of Cr(VI) ions from the aqueous solution.
(iii) The adsorption isotherm data were better described by the Redlich–Peterson model.
(iv) The Langmuir maximum monolayer adsorption capacity of the SMSP for the removal of Cr(VI) ions was found to be of 202.7 mg/g.
(v) The adsorption thermodynamic parameters indicated that the adsorption of Cr(VI) ions onto RSP and SMSP was spontaneous and exothermic in nature of adsorption.
(vi) The adsorption kinetics was found to follow the pseudo-first-order kinetic model.
(vii) The influence of other salts such as NH_4Cl, NH_4NO_3, KNO_3, $MgSO_4$, $NaHCO_3$ and $K_2P_2O_7$ in removal of Cr(VI) ions was studied.
(viii) The desorption of Cr(VI) ions from the spent adsorbent was studied by the help of different desorbents such as H_2SO_4, HCl, HNO_3, HCHO, KOH and NaOH. The desorption results

showed that the preferred desorbent for the present desorption system was of NaOH.

(ix) In column adsorption process, the operating parameters such as bed height (2–10 cm), Cr (VI) ions concentration (50–250 mg/L) and flow rate (5–25 mL/min) were studied and optimized for the maximum removal of Cr(VI) ions.

(x) The column adsorption results were best described by the Thomas and BDST models.

The adsorption results indicated that the prepared SMSP is an efficient adsorbent for the removal of Cr(VI) ions from the aqueous solution.

References

[1] M.J. Udy, Chromium, Reinhold Publishing Corporation, New York, NY, 1956.

[2] L.J. Casarett, J. Doul, Toxicology, the Basic Science of Poisons, Macmillan, New York, NY, 1980.

[3] R. Zhang, B. Wang, H. Ma, Studies on Chromium (VI) adsorption on sulfonated lignite, Desalination 255 (2010) 61–66.

[4] J.O. Nriagu, E. Nriagu, Chromium in the Natural and Human Environment, Wiley, New York, NY, 1988.

[5] X. Jing, Y. Cao, X. Zhang, D. Wang, X. Wu, H. Xu, Biosorption of Cr(VI) from simulated wastewater using a cationic surfactant modified spent mushroom, Desalination 269 (2011) 120–127.

[6] K. Mohanty, M. Jha, B.C. Meikap, M.N. Biswas, Removal of chromium (VI) from dilute aqueous solutions by activated carbon developed from *Terminalia arjuna* nuts activated with zinc chloride, Chem. Eng. Sci. 60 (2005) 3049–3059.

[7] P.A. Kumar, S. Chakraborty, Fixed-bed column study for hexavalent chromium removal and recovery by short-chain polyaniline synthesized on jute fiber, J. Hazard. Mater. 162 (2009) 1086–1098.

[8] A.G. Yavuz, E. Dincturk-Atalay, A. Uygun, F. Gode, E. Aslan, A comparison study of adsorption of Cr(VI) from aqueous solutions onto alkyl-substituted polyaniline/chitosan composites, Desalination 279 (2011) 325–331.

[9] A.K. Meena, K. Kadirvelu, G.K. Mishra, C. Rajagopal, P.N. Nagar, Adsorptive removal of heavy metals from aqueous solution by treated sawdust (*Acacia arabica*), J. Hazard. Mater. 150 (2008) 604–611.

[10] C.A. Basha, K. Ramanathan, R. Rajkumar, M. Mahalakshmi, P.S. Kumar, Management of chromium plating rinsewater using electrochemical ion exchange, Ind. Eng. Chem. Res. 47 (2008) 2279–2286.

[11] P.S. Kumar, K. Kirthika, K.S. Kumar, Removal of hexavalent chromium ions from aqueous solutions by an anion-exchange resin, Adsorpt. Sci. Technol. 26 (2008) 693–703.

[12] P.S. Kumar, K. Kirthika, K.S. Kumar, Bael tree leaves as a natural adsorbent for the removal of zinc(II) ions from industrial effluents, Adsorpt. Sci. Technol. 27 (2009) 503–512.

[13] BIS, Methods of Sampling and Test (Physical and Chemical) for Water and Waste water: Part 52 Chromium, IS No. 3025 (Part 52), 2003.

[14] P. SenthilKumar, S. Ramalingam, V. Sathyaselvabala, S.D. Kirupha, S. Sivanesan, Removal of copper(II) ions from aqueous solution by adsorption using cashew nut shell, Desalination 266 (2011) 63–71.

[15] P.S. Kumar, S. Ramalingam, S.D. Kirupha, A. Murugesan, T. Vidhyadevi, S. Sivanesan, Adsorption behavior of nickel(II) onto cashew nut shell: Equilibrium, thermodynamics, kinetics, mechanism and process design, Chem. Eng. J. 167 (2011) 122–131.

[16] P. SenthilKumar, S. Ramalingam, R.V. Abhinaya, S.D. Kirupha, T. Vidhyadevi, S. Sivanesan, Adsorption equilibrium, thermodynamics, kinetics, mechanism and process design of zinc(II) ions onto cashew nut shell, Can. J. Chem. Eng. 90 (2012) 973–982.

[17] P.S. Kumar, S. Ramalingam, R.V. Abhinaya, K.V. Thiruvengadaravi, P. Baskaralingam, S. Sivanesan, Lead(II) adsorption onto sulphuric acid treated cashew nut shell, Sep. Sci. Technol. 46 (2011) 2436–2449.

[18] P. Senthil Kumar, S. Ramalingam, R.V. Abhinaya, S.D. Kirupha, A. Murugesan, S. Sivanesan, Adsorption of metal ions onto the chemically modified agricultural waste, CLEAN – Soil, Air, Water 40 (2012) 188–197.

[19] P.S. Kumar, S. Ramalingam, V. Sathyaselvabala, S.D. Kirupha, A. Murugesan, S. Sivanesan, Removal of cadmium(II) from aqueous solution by agricultural waste cashew nut shell, Korean J. Chem. Eng. 29 (2012) 756–768.

[20] P. Rajkumar, P. Senthil Kumar, S. Dinesh Kirupha, T. Vidhyadevi, J. Nandagopal, S. Sivanesan, Adsorption of Pb(II) ions onto surface modified *Guazuma ulmifolia* seeds and batch adsorber design, Environ. Prog. Sustainable Energy 32 (2013) 307–316.

[21] P.S. Kumar, R. Gayathri, C. Senthamarai, M. Priyadharshini, P.S.A. Fernando, R. Srinath, V.V. Kumar, Kinetics, mechanism, isotherm and thermodynamic analysis of adsorption of cadmium ions by surface-modified *Strychnos potatorum* seeds, Korean J. Chem. Eng. 29 (2012) 1752–1760.

[22] P. Senthil Kumar, C. Senthamarai, A. Durgadevi, Adsorption kinetics, mechanism, isotherm, and thermodynamic analysis of copper ions onto the surface modified agricultural waste, Environ. Prog. Sustainable Energy 33 (2014) 28–37.

[23] P. Senthil Kumar, C. Senthamarai, A.S.L. Sai Deepthi, R. Bharani, Adsorption isotherms, kinetics and mechanism of Pb(II) ions removal from aqueous solution using chemically modified agricultural waste, Can. J. Chem. Eng. 91 (2013) 1950–1956.

[24] P. Senthil Kumar, Adsorption of lead(II) ions from simulated wastewater using natural waste: A kinetic, thermodynamic and equilibrium study, Environ. Prog. Sustainable Energy 33 (2014) 55–64.

[25] D. Park, S.-R. Lim, Y.-S. Yun, J.M. Park, Development of a new Cr(VI)-biosorbent from agricultural biowaste, Bioresour. Technol. 99 (2008) 8810–8818.

[26] H. Gao, Y. Liu, G. Zeng, W. Xu, T. Li, W. Xia, Characterization of Cr(VI) removal from aqueous solutions by a surplus agricultural waste—Rice straw, J. Hazard. Mater. 150 (2008) 446–452.

[27] V.K. Gupta, A. Rastogi, Biosorption of hexavalent chromium by raw and acidtreated green alga Oedogonium hatei from aqueous solutions, J. Hazard. Mater. 163 (2009) 396–402.
[28] J.R. Memon, S.Q. Memon, M.I. Bhanger, A. El-Turki, K.R. Hallam, G.C. Allen, Banana peel: A green and economical sorbent for the selective removal of Cr(VI) from industrial wastewater, Colloids Surf., B 70 (2009) 232–237.
[29] R. Elangovan, L. Philip, K. Chandraraj, Biosorption of hexavalent and trivalent chromium by palm flower (*Borassus aethiopum*), Chem. Eng. J. 141 (2008) 99–111.
[30] G. Rojas, J. Silva, J.A. Flores, A. Rodriguez, M. Ly, H. Maldonado, Adsorption of chromium onto cross-linked chitosan, Sep. Purif. Technol. 44 (2005) 31–36.
[31] K.Z. Elwakeel, Environmental application of chitosan resins for the treatment of water and wastewater: A review, J. Dispersion Sci. Technol. 31 (2010) 273–288.
[32] V.A. Spinelli, M.C.M. Laranjeira, V.T. Fávere, Preparation and characterization of quaternary chitosan salt: Adsorption equilibrium of chromium(VI) ion, React. Funct. Polym. 61 (2014) 347–352.
[33] D.P. Mungasavalli, T. Viraraghavan, Y.-C. Jin, Biosorption of chromium from aqueous solutions by pretreated Aspergillus niger: Batch and column studies, Colloids Surf., A 301 (2007) 214–223.
[34] F. Gode, E.D. Atalay, E. Pehlivan, Removal of Cr(VI) from aqueous solutions using modified red pine sawdust, J. Hazard. Mater. 152 (2008) 1201–1207.
[35] V.K. Garg, R. Gupta, R. Kumar, R.K. Gupta, Adsorption of chromium from aqueous solution on treated sawdust, Bioresour. Technol. 92 (2004) 79–81.
[36] R. Chand, K. Narimura, H. Kawakita, K. Ohto, T. Watari, K. Inoue, Grape waste as a biosorbent for removing Cr(VI) from aqueous solution, J. Hazard. Mater. 163 (2009) 245–250.
[37] K.K. Singh, S.H. Hasan, M. Talat, V.K. Singh, S.K. Gangwar, Removal of Cr(VI) from aqueous solutions using wheat bran, Chem. Eng. J. 151 (2009) 113.
[38] V. Prigione, M. Zerlottin, D. Refosco, V. Tigini, A. Anastasi, G.C. Varese, Chromium removal from a real tanning effluent by autochthonous and allochthonous fungi, Bioresour. Technol. 100 (2009) 2770–2776.
[39] O. Maryuk, S. Pikus, E. Olszewska, M. Majdan, H. Skrzypek, E. Zieba, Benzyldimethyloctadecylammonium bentonite in chromates adsorption, Mater. Lett. 59 (2005) 2015–2017.
[40] F. Granados-Correa, J. Jiménez-Becerril, Chromium (VI) adsorption on boehmite, J. Hazard. Mater. 162 (2009) 1178–1184.
[41] Y. Bayrak, Y. Yesiloglu, U. Gecgel, Adsorption behavior of Cr(VI) on activated hazelnut shell ash and activated bentonite, Microporous Mesoporous Mater. 91 (2006) 107–110.
[42] M. Noroozifar, M. Khorasani-Motlagh, M.N. Gorgij, H.R. Naderpour, Adsorption behavior of Cr(VI) on modified natural zeolite by a new bolaform N, N, N, N′, N′, N′-hexamethyl-1,9-nonanediammonium dibromide reagent, J. Hazard. Mater. 155 (2008) 566–571.
[43] M. Majdan, S. Pikus, Z. Rzączyńska, M. Iwan, O. Maryuk, R. Kwiatkowski, H. Skrzypek, Characteristics of chabazite modified by hexadecyltrimethylammonium bromide and of its affinity toward chromates, J. Mol. Struct. 791 (2006) 53–60.
[44] K. Barquist, S.C. Larsen, Chromate adsorption on amine-functionalized nanocrystalline silicalite-1, Microporous Mesoporous Mater. 116 (2008) 365–369.
[45] L. Bois, A. Bonhommé, A. Ribes, B. Pais, G. Raffin, F. Tessier, Functionalized silica for heavy metal ions adsorption, Colloids Surf., A 221 (2003) 221–230.
[46] J.S. Li, X.Y. Miao, Y.X. Hao, J.Y. Zhao, X.Y. Sun, L.J. Wang, Synthesis, aminofunctionalization of mesoporous silica and its adsorption of Cr(VI), J. Colloid Interface Sci. 318 (2008) 309–314.
[47] J.S. Noh, J.A. Schwarz, Estimation of the point of zero charge of simple oxides by mass titration, J. Colloid Interface Sci. 130 (1989) 157–164.
[48] I. Langmuir, The adsorption of gases on plane surfaces of glass, mica and platinum, J. Am. Chem. Soc. 40 (1918) 1361–1403.
[49] H.M.F. Freundlich, Over the adsorption in solution, J. Phys. Chem. 57 (1906) 385–470.
[50] O. Redlich, D.L. Peterson, A useful adsorption isotherms, J. Phys. Chem. 63 (1959) 1024–1026.
[51] R. Sips, On the structure of a catalyst surface, J. Phys. Chem. 16 (1948) 490–495.
[52] S. Lagergren, About the theory of so-called adsorption of soluble substances, Kungliga Svenska Vetensk Handl. 24 (1898) 1–39.
[53] Y.S. Ho, G. McKay, Pseudo-second order model for sorption processes, Process Biochem. 34 (1999) 451–465.
[54] M.J.D. Low, Kinetics of chemisorption of gases on solids, Chem. Rev. 60 (1960) 267–312.
[55] S. Kundu, A.K. Gupta, Analysis and modeling of fixed bed column operations on As (V) removal by adsorption onto iron oxide-coated cement (IOCC), J. Colloid Interface Sci. 290 (2005) 52–60.
[56] H.C. Thomas, Heterogeneous ion exchange in a flowing system, J. Am. Chem. Soc. 66 (1944) 1466–1664.
[57] R.A. Hutchins, New method simplifies design of activated carbon systems, Chem. Eng. 80 (1973) 133–138.
[58] K.R. Eagleton, L.C. Acrivers, T. Vermenlem, Pore and solid diffusion kinetics in fixed adsorption constant pattern conditions, Ind. Eng. Chem. Res. 5 (1966) 212–223.
[59] G. McKay, M.S. Otterburn, A.G. Sweetney, The removal of colour from effluent using various adsorbents-III. Silica: Rate processes, Water Res. 14 (1981) 14–20.
[60] D. Das, G. Basak, V. Lakshmi, N. Das, Kinetics and equilibrium studies on removal of zinc (II) by untreated and anionic surfactant treated dead biomass of yeast: Batch and column mode, Biochem. Eng. J. 64 (2012) 30–47.
[61] P. Suksabye, P. Thiravetyan, Cr(VI) adsorption from electroplating plating wastewater by chemically modified coir pith, J. Environ. Manage. 102 (2012) 1–8.
[62] A. Kurniawan, A.N. Kosasih, J. Febriano, Y.H. Ju, J. Sunarso, N. Indraswati, Evaluation of cassava peel waste as lowcost biosorbent for Ni sorption: Equilibrium, kinetics, thermodynamics and mechanisms, Chem. Eng. J. 172 (2011) 158–166.
[63] M. Arulkumar, K. Thirumalai, P. Sathishkumar, T. Palvannan, Rapid removal of chromium from aqueous solution using novel prawn shell activated carbon, Chem. Eng. J. 185,186 (2012) 178–186.
[64] A.R. Netzahuatl-Muñoz, F.D.M. Guillén-Jiménez, B. Chávez-Gómez, T.L. Villegas-Garrido, E. Cristiani-Urbina, Kinetic study of the effect of pH on hexavalent

and trivalent chromium removal from aqueous solution by *Cupressus lusitanica* bark, Water Air Soil Pollut. 223 (2012) 625–641.
[65] A.B. Albadarin, A.H. Al-Muhtaseb, G.M. Walker, S.J. Allen, M.N.M. Ahmad, Retention of toxic chromium from aqueous phase by H3PO4-activated lignin: Effect of salts and desorption studies, Desalination 274 (2011) 64–73.
[66] A.A. Muxel, S.M.N. Gimenez, F.A.S. Almeida, R.V.S. Alfaya, A.A.S. Alfaya, Cotton fiber/ZrO_2, a new material for adsorption of Cr(VI) ions in water, CLEAN - Soil, Air, Water 39 (2011) 289–295.
[67] S. Mor, K. Ravindra, N.R. Bishnoi, Adsorption of chromiumfromaqueous solution by activated alumina and activated charcoal, Bioresour. Technol. 98 (2007) 954–957.
[68] C. Namasivayam, D. Sangeetha, Removal of chromium(VI) by $ZnCl_2$ activated coir pith carbon, Toxicol. Environ. Chem. 88 (2006) 219–233.
[69] M. Dakiky, M. Khamis, M. Manassra, M. Mereb, Selective adsorption of Chromium(VI) in industrial waste water using low cost abundantly available adsorbents, Adv. Environ. Res. 6 (2002) 533–540.
[70] D. Mohan, K.P. Singh, V.K. Singh, Using low-cost activated carbons derived from agricultural waste materials and activated carbon fabric cloth, Ind. Eng. Chem. Res. 44 (2005) 1027–1042.
[71] X.-J. Hu, J.-S. Wang, Y.-G. Liu, X. Li, G.-M. Zeng, Z.-L. Bao, X.-X. Zeng, A.-W. Chen, F. Long, Adsorption of chromium (VI) by ethylenediamine-modified cross-linked magnetic chitosan resin: Isotherms, kinetics and thermodynamics, J. Hazard. Mater. 185 (2011) 306–314.
[72] V. Singh, S. Tiwari, A.K. Sharma, R. Sanghi, Removal of lead from aqueous solutions using *Cassia grandis* seed gum-graft-poly(methylmethacrylate), J. Colloid Interface Sci. 316 (2007) 224–232.